Order Number 9503594

Optical and magnetic resonance studies of novel pristine and photo-oxidized conjugated polymers

Smith, Andrew Vernon, Ph.D.

Iowa State University, 1994

U·M·I
300 N. Zeeb Rd.
Ann Arbor, MI 48106

Optical and magnetic resonance studies of novel pristine and photo-oxidized conjugated polymers

by

Andrew Vernon Smith

A Dissertation Submitted to the

Graduate Faculty in Partial Fulfillment of the

Requirements for the Degree of

DOCTOR OF PHILOSOPHY

Department: Physics and Astronomy
Major: Condensed Matter Physics

Approved:

Signature was redacted for privacy.

In Charge of Major Work

Signature was redacted for privacy.

For the Major Department

Signature was redacted for privacy.

For the Graduate College

Iowa State University
Ames, Iowa

1994

TABLE OF CONTENTS

INTRODUCTION

Rapid advances in the development of π-conjugated polymer-based LEDs[1-8] and the present challenges to improve their stability and efficiency provide a strong motivation for basic studies of their photo- and device-physics. Light emitting diode displays are being marketed in a wide variety of solid state electronic components today. Television, radio and computer display panels are among the most prominent of those everyday appliances employing LEDs. Most of the LEDs with which efficient light generation has been achieved and developed until now have used inorganic III-V compounds such as GaAs or II-VI compounds such as ZnS. GaAs devices, however, have proven to be difficult to manufacture easily and economically as large area displays. Though somewhat less expensive, polycrystalline ZnS devices provide low efficiency and poor reliability. The advent of large scale research into the use of organic molecular semiconductors was brought on by the fact that they generally exhibit high photoluminescence (PL) quantum yields.

Improved structural stability can be achieved in organic layers by moving from molecular to macromolecular materials such as conjugated polymers. Poly(*p*-phenylene-vinylene) (PPV) has shown the most promise[1] though research is ongoing into other polymers such as poly(3-hexylthiophene) (P3HT)[5] and poly(*p*-phenyleneacetylene) (PPA).[9] As unsubstituted PPV is an insoluble and brittle material, high quality films of sufficient purity to control the nonradiative decay of excited states at defect sites in this polymer have been achieved via a solution-processible precursor.

Electroluminescing structures can be formed using a glass substrate with a semi-transparent film of indium-tin-oxide (ITO) deposited on one surface. The polymer solution is then spin-coated onto the ITO. A small portion of the ITO surface must be uncovered for attachment of an electrical contact. Another metallic contact (i.e., aluminum) is evaporated onto the top surface of the polymer layer. When a bias is applied, the electroluminescent properties of the device can be studied. An example of a polymer-based LED structure is shown in Figure 1. Note that no direct work on these devices has been done and shown in this thesis. However, the data and results shown here have been motivated by and are indirectly associated with the ongoing research effort into the development of polymer-based LEDs.

In the early years of polymer technology, the sole uses of these organic compounds were as insulators (ie., the electrical conductivities were poor). The onset of conducting, dopable or semiconducting polymers occurred in 1977 when Chiang et al[10] showed that the conductivity of polyacetylene could be drastically improved through doping to as high as 10^4 S/cm. Polyacetylene, as well as all other polymers, can be modeled as a quasi-one-dimensional system which features the very important π molecular orbitals delocalized along the chain. The half-filled band of polyacetylene leads to a dimerization of successive sites along the chain.[11] This dimerization produces an energy gap and renders the polymer a semiconductor. In 1979-80, Su, Schrieffer and Heeger[12,13] successfully modeled the semiconducting properties of this degenerate ground state polymer to show that solitons, and not electrons and holes, are the primary excitation. Subsequent theories of other novel

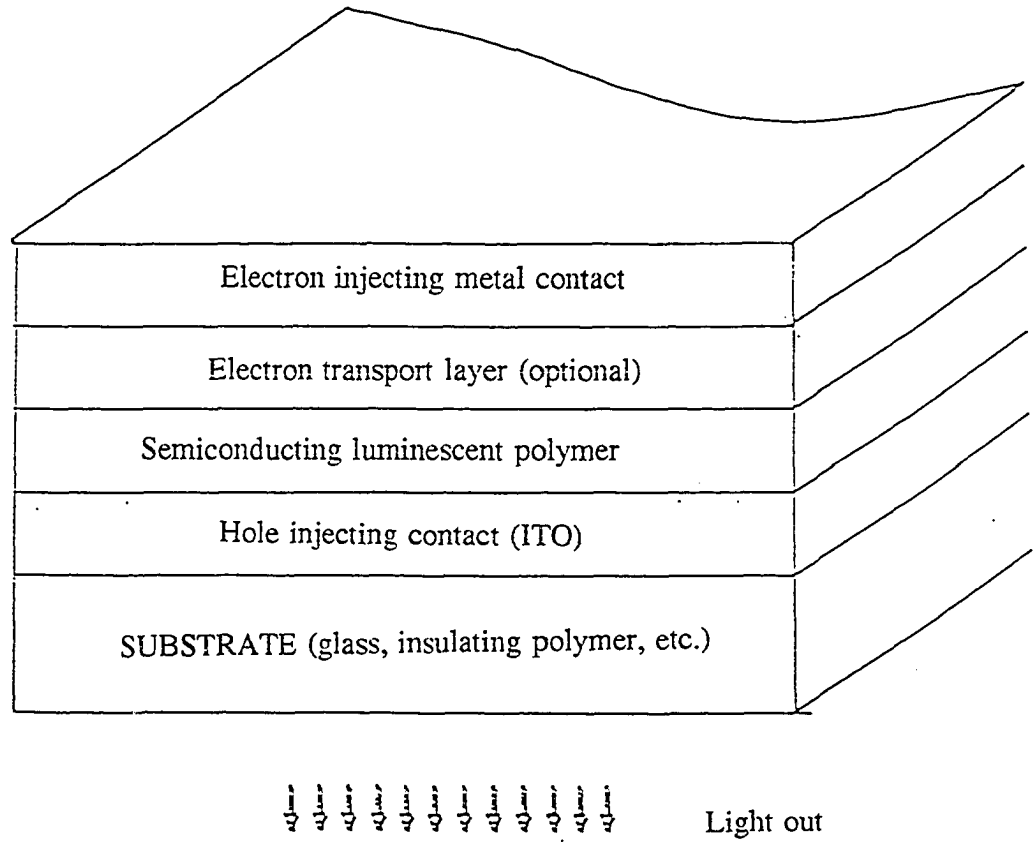

Figure 1
Structure of the polymer LED

nondegenerate ground state conjugated polymers such as polythiophene (PT) and poly(*p*-phenylenevinylene) (PPV) have attributed a similar role to excitons, polarons, and bipolarons.[14,15]

The polymers studied here and which are shown in Figures 2-6 in the pictorial notation of organic chemistry include: poly(*p*-phenyleneethynyleneaniline) and its derivatives, poly(*p*-phenylenevinylene) in several different forms, poly(3-hexylthiophene), poly(2,5-dibutoxyparaphenyleneethynylene), poly(*p*-phenylenecumulene) in different forms and poly(*p*-di(phenyleneethynylene)phenylenevinylene). We now consider the elements that make up a polymer and discuss their independent significance.

Perhaps the most important property is the orbital hybridization responsible for the delocalization which brings forth the high conducting nature of these polymers. Carbon has three hybridization schemes: sp, sp^2 and sp^3. The hybrid sp orbital yields two π electrons and the hybrid sp^2 orbital yields one. The sp^3 scheme which is most usual in carbon compounds has four σ bonds associated with its four valence electrons. A good example of sp^3 hybridization is methane, CH_4 , in which each hydrogen is σ bonded to the central carbon in a tetrahedral arrangement (see Figure 7). A most important example of the sp^2 scheme is ethylene(vinylene), C_2H_4, which is depicted in Figure 7. In this case, the carbon-carbon and carbon-hydrogen σ bonds all lie in the x-y plane. Each carbon atom has an additional electron which forms a π bond between them. The π orbitals are aligned along the z direction and form an electron cloud which is delocalized over the length of the entire molecule. Any distortion of the planar nature of the σ bonds of this molecule would break the π bond and

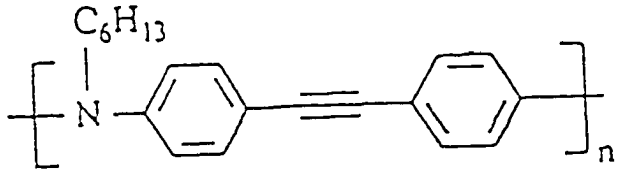

poly(*p*-phenyleneethynyleneaniline)
(PPEA)

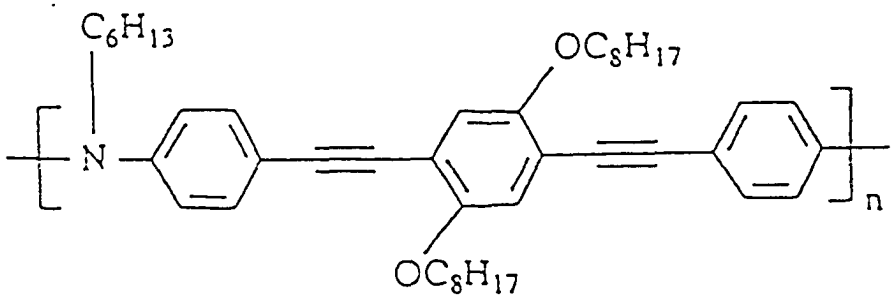

poly(di(phenyleneethynylene)aniline)
(PDPEA)

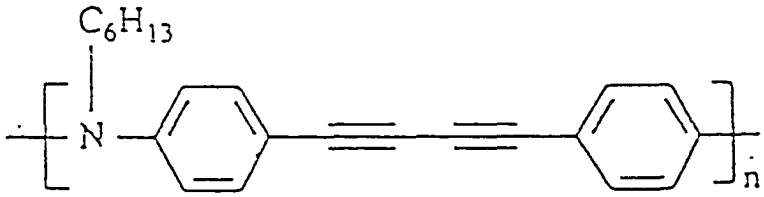

poly(phenylenedi(ethynylene)aniline)
(PPDEA)

Figure 2
Poly(p-phenyleneethynyleneaniline)
derivatives

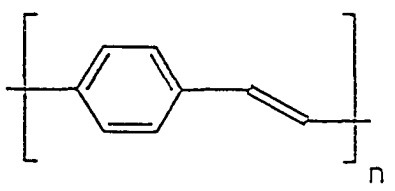

poly(p-phenylene-vinylene)

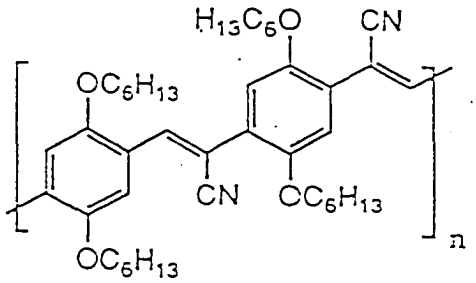

Poly(cyano-p-phenylene-vinylene)

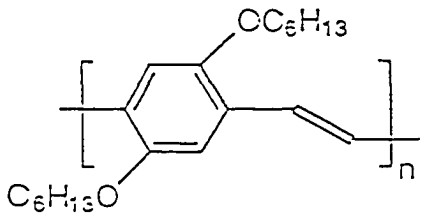

poly(2,5-dihexoxy-*p*-phenylene-vinylene)

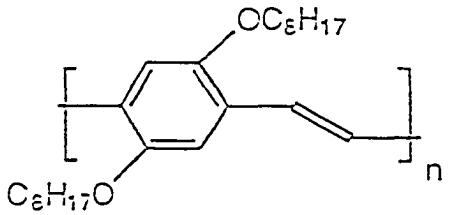

Poly(2,5-dioctoxy-*p*-phenylene-vinylene)

Figure 3
Poly(p-phenylenevinylene)
and substituted derivatives

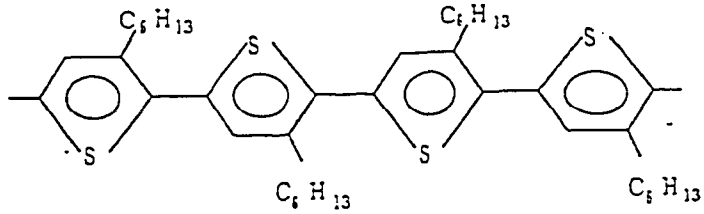

Poly(3-hexylthiophene)

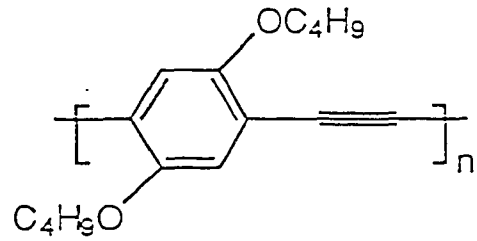

poly(2,5-dibutoxy-p-phenylene-ethynylene)

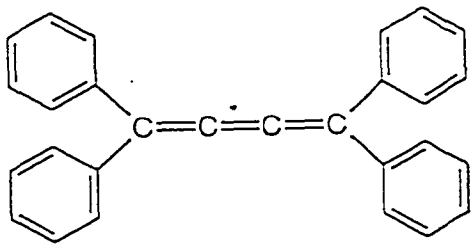

1,1,4,4-tetraphenyl-1,2,3-butatriene

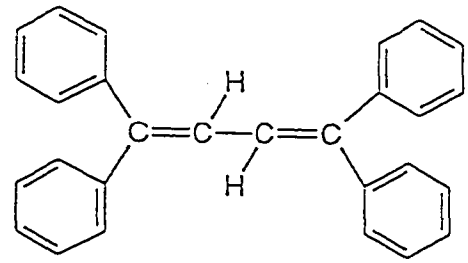

1,1,4,4,-tetraphenyl-1,3-butadiene

Figure 4
P3HT, PDBOPA and
polycumulene monomers

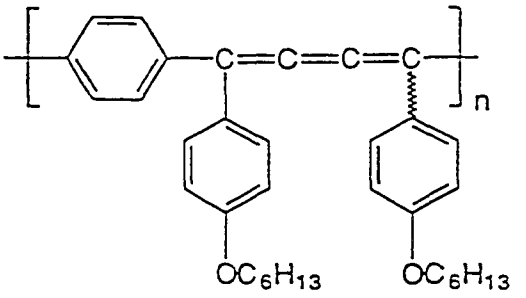

poly(p-phenylene-1,4-bis(p-hexoxyphenyl)-1,2,3-butatriene)

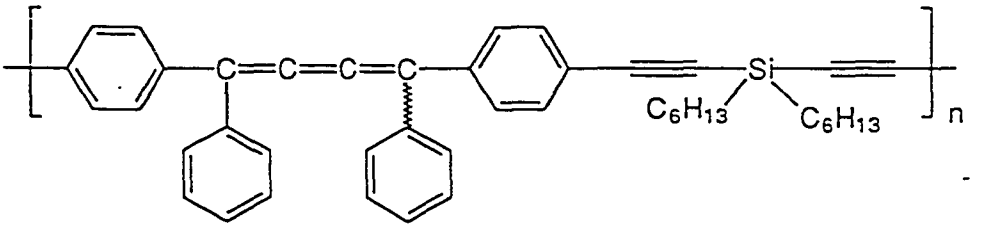

poly(p-phenylene-1,4-diphenyl-1,2,3-butatriene-p-phenylene-ethynylene-dihexylsilylene-ethynylene)

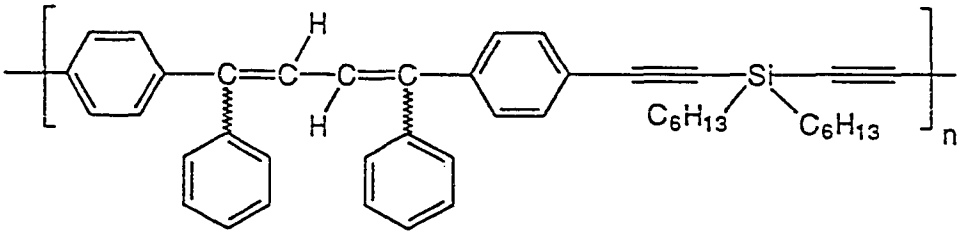

poly(p-phenylene-1,4-diphenyl-1,3-butadiene-p-phenylene-ethynylene-dihexylsilylene-ethynylene)

Figure 5
Substituted polycumulene and
alternative polycumulenes

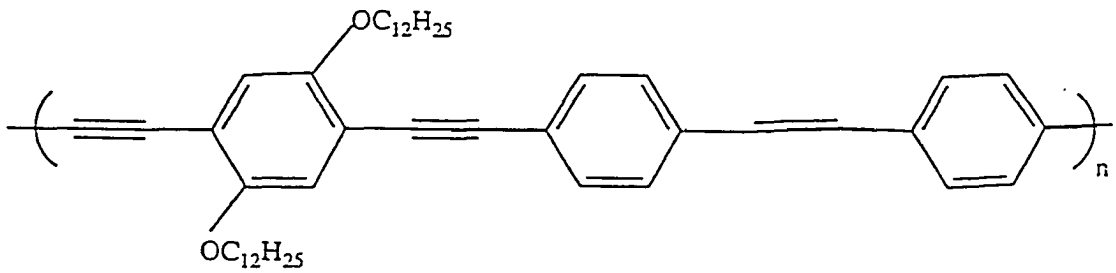

poly(diphenyleneethynylene-phenylene-vinylene) (PDPEPV)

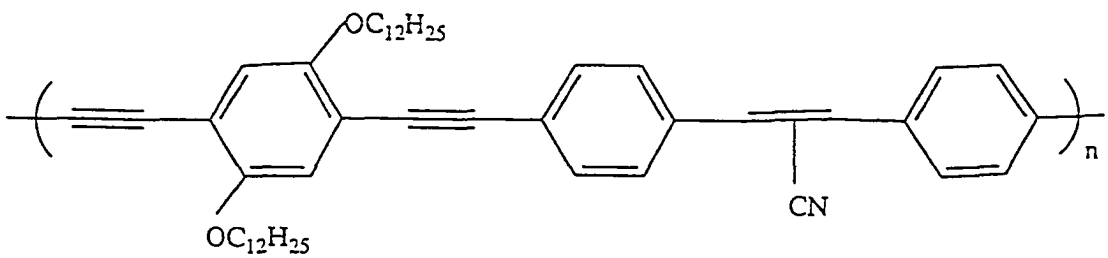

poly(diphenyleneethynylene-phenylene-cyano-vinylene) (PDPEPCV)

Figure 6
PDPEPV and cyano
substituted PDPEPV

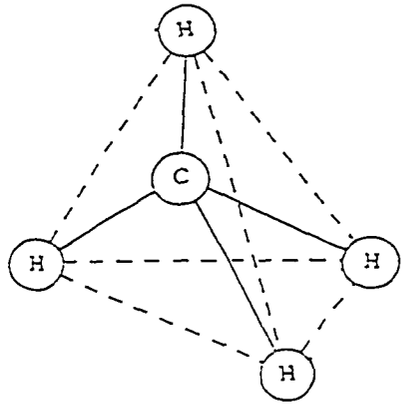

Methane

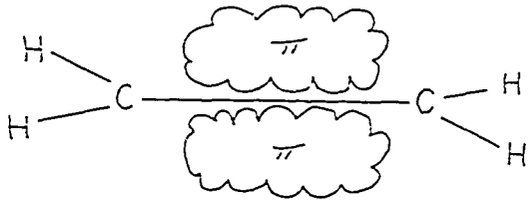

Ethylene(vinylene)

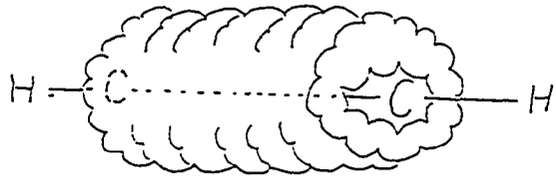

Ethynylene(acetylene)

Figure 7
Methane, ethylene and
ethynylene (acetylene)

disrupt the molecular π orbital. In fact, the conjugation length of a polymer, whose significance will be discussed later, depends on how well the σ bonded elements remain in the x-y plane and allow the z direction to contain undisturbed molecular π orbitals. The most significant example, for our purposes, of an sp hybridized molecule is acetylene (ethynylene), C_2H_2 . In this case, each carbon atom is σ bonded to a hydrogen and the other carbon leaving two π bonds between the carbon atoms. The σ bonds are collinear along the x-axis. The π electrons are in linear combinations of states in the y and z directions and thus form a cylindrical cloud around the C-C axis (see Figure 7).

The next important group of elements to consider are aromatic rings (Figure 8). These differ from the ethylene and acetylene units in that the central component is a ring of six atoms (at least five carbons). Each atom bonds to each of its two neighbors and a hydrogen atom leaving one electron per carbon to be delocalized in a π cloud which lies above and below the plane of the ring. The most obvious example of an aromatic ring is benzene (or phenylene). A benzene ring is completely symmetrical having six carbons comprising its hexagonal matrix. The actual pairs of carbon atoms between which the π bonds exist are unknown because the energy of either of the two possible configurations is the same. In fact, all of the carbon-carbon bond distances are equal.[16] Furthermore, the carbon-carbon bond angles are all exactly 120°. Thus, since three distinct carbon-carbon double bonds will not be formed, the six π electrons from the six carbon atoms will form a continuous π electron cloud that is symmetrical and coplanar with the plane of the hexagonal ring. It should be noted that since no more than two electrons can occupy a single π orbital, the figure should not be

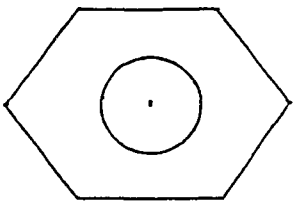

Benzene(phenylene)

The two configurations of Benzene

Thiophene Furan

Figure 8
Aromatic rings including benzene
and its two possible bonding configurations

considered a single π orbital containing six electrons. Rather, there must be three π orbitals present in the π electron cloud.[16] Some other examples of aromatic structures are shown along with benzene in Figure 8.

A polymer consists of repeat units linked together in a chain. The related monomers may be composed of aromatic rings, ethylene molecules, acetylene units, single carbon or nitrogen atoms and/or a variety of other atomic or molecular ingredients. The π electrons associated with each element further delocalize in this arrangement over several molecular units. They are able to be delocalized over a segment of the chain which is completely planar. A point at which there is a kink in the chain marks a point at which a π bond may be broken and the extended electron cloud edge defined. The length between the nearest two of these defects in the chain is the conjugation length. The bandgap of the polymer is directly related to the degree of localization of the π electrons and thus inversely so to the conjugation length. Too many twists or bends along the chain will cause the polymer to become an insulator due to its high gap.

Su, Schrieffer and Heeger[15] first predicted the existence of states lying in the gap. Some of these states into which π electrons can be photo-excited include polarons, bipolarons and excitons. A polaron (see Figure 9) is an electron (or hole) which couples to the lattice around it. This electron-phonon interaction lowers the electron's energy and produces a state in the gap. The effective mass of the electron (hole) is seen to increase as it "drags the heavy ion cores around with it"[17]. At room temperature, the electron-phonon interaction is responsible for electrical resistivity in metals. When the electron (hole) strongly interacts with

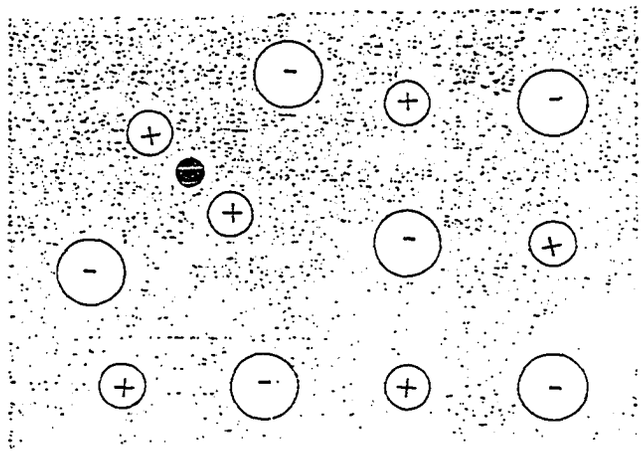

Negative polaron

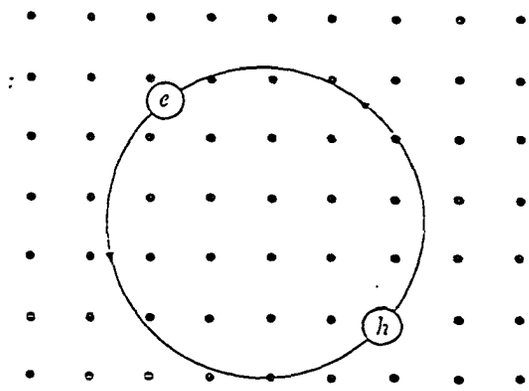

Exciton

Figure 9
Schematic representations of a polaron and an exciton in possible lattice configurations[17]

the strain field of the lattice, it can become self trapped as in ionic crystals where the coulomb interaction is great and the electrical conductivity is low. Spinless bipolarons are formed between two like charged species because the energy is lower than that of two independent polarons. Bipolarons are significant independent excitations as shall be discussed later. Finally, a bound electron-hole pair is known as an exciton. Excitons can exist in singlet and triplet states. Excitonic states lie in the gap because of their binding energy. Singlet excitons are unstable species which decay readily. It is generally agreed that it is the decay of singlet excitons that is responsible for the bulk photoluminescence (PL) in most semiconducting materials. Excitons can be formed by photon absorption at energies less than the bandgap of the polymer or by relaxation of electrons and holes into bound states. Binding energies of excitons have been measured from absorption and luminescence measurements. Some excitons are tightly bound, possibly localized on a single atom. Others are more weakly bound with average electron-hole distances much greater than a lattice constant (see Figure 9). Triplet excitons differ from singlets in that the spins of the charge carrying components are aligned parallel. Obviously, radiative recombination of triplet excitons is not allowed in first order. Consequently, observing these events is less common than simply measuring the PL. However, using the technique of optically detected magnetic resonance (ODMR), to be described later, unmistakable signatures of triplet excitons in conjugated polymers will be shown.

The novelty of the approach taken in this study resides in the use of ultraviolet excitation for the ODMR and PL measurements. The original reason for doing this was in

order to be able to excite electrons into excited states in polymers whose bandgaps are too high for visible, laser energies. The results obtained on the poly(p-phenyleneethynylene-aniline) (PPEA) derivatives is an example of the usefulness of this idea. The most interesting result of using ultraviolet excitation, however, was achieved by reexaming polymers which had been previously studied using visible laser excitation. New ODMR signatures were found which have given valuable insight into the nature of excited states in conjugated polymers.

Photoluminescence (PL)

Radiative absorption takes place in a material when an incident photon gives up its energy to an electron which then jumps into an excited state. The emission of radiation is the inverse of the absorption process. The fundamental difference is that absorption can involve all of the states on either side of the Fermi level whereas emission is usually due to transitions between electrons in a narrow band of excited states and a narrow band of holes. Therefore, emission spectra tend to be narrower than absorption spectra.

Photoluminescence is light emission from semiconducting materials due to the radiative decay of excited states whose existence was brought about by the absorption of photons by the ground state of the material. Two types of PL are generally distinguished: florescence and phosphorescence. Florescence is a fast (up to ~0.1 μs) process, usually associated with processes allowed by the selection rules. Phosphorescence is a slower (longer than 1 μs) process which is usually associated with forbidden transitions, e.g., decay of

triplets. The radiative efficiency depends on whether competing processes involving intermediate states (see Figure 10) exist. The intermediate state clearly does not participate in the absorption of the incident photon. However, there are two competing processes for recombination. The transition involving the intermediate state may or may not involve photon emission, but if it does, the photon will have less energy than hν. The probability term in the radiation rate equation is then reduced due to the extra contribution to the reciprocal of the recombination lifetime due to the existence of the second recombination path.

The fundamental radiative transition involved in the photoluminescence of semiconductors is generally accepted to be from the decay of singlet excitons. The energies of the emitted photons are less than the energy gap of the semiconductor by an amount equal to the binding energy of the exciton plus the energy of any phonons emitted in the process. Considering the exciton as a positronium-like excitation, it could be in any of a series of excited states whose binding energies decrease as $\mathbf{1/n^2}$. However the intensity of the higher order transition rates decreases as $\mathbf{1/n^3}$ [19]. Phonons may be emitted in a direct process and must be emitted in an indirect one. Phonon emission occurs, however, at the expense of a lower transition probability. Thus, in general, the energy of the emitted photon in a process involving the decay of a singlet exciton can be described as:

$$\mathbf{h\nu = E_{gap} - (1/n^2)E_{binding} - pE_{phonon}}$$

where **n** is the excited state quantum number for the exciton and **p** is the number of phonons emitted of energy $\mathbf{E_{phonon}}$. Note that the highest

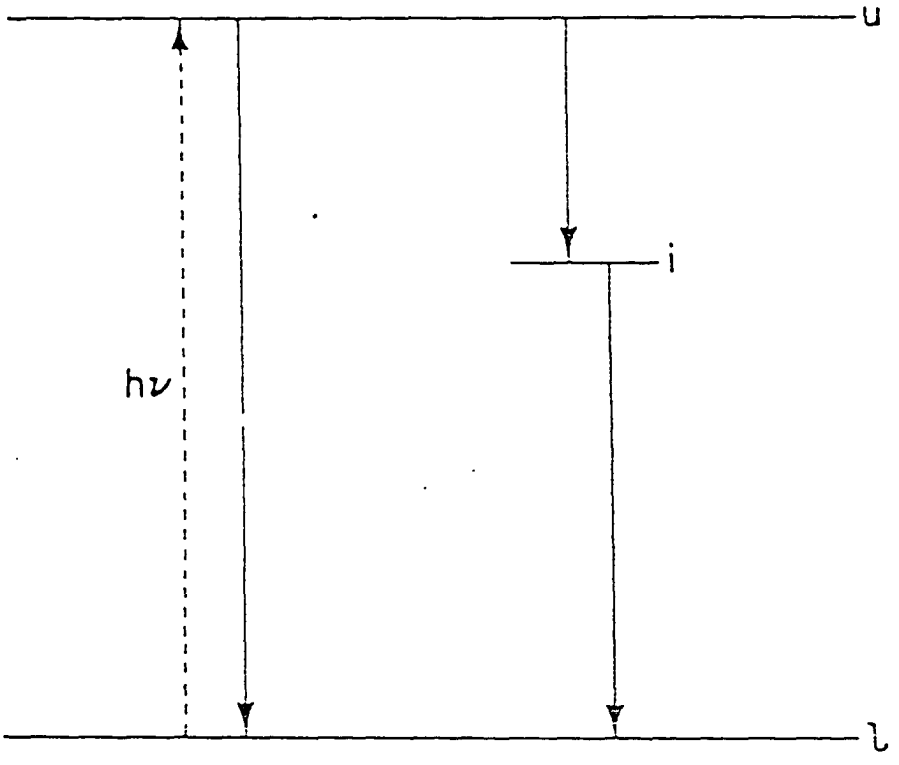

Figure 10
Schematic representation of
two competing recombination processes[18]

transition probability corresponds to when **n** = 1 and **p** = 0 for direct gap semiconductors and **p** = 1 for indirect ones (see Figure 11).

Bound excitons may exist in a material which has impurities. The photon emission from the decay of these excitons differs from that of free excitons as they occur at lower energy and have a narrower line width.

Band-to-band transitions can take place between free carriers occupying band states. The emitted photon energies will be at least the gap energy in contrast to the lower energy exciton decay processes. Even in the purest materials where excitons are easily formed, there will be a number of free carriers occupying band states. In less pure crystals, free excitons are broken up by local fields yielding more free carriers and reducing the number of free excitons available for radiative decay. These free carriers can themselves recombine radiatively, however, in band-to-band transitions.

Some conjugated polymers have a strong photoluminescence and others do not luminesce at all. There has been much discussion as to how it can be determined, without direct experimental evidence, whether a novel polymer will luminesce. Since this seems to be a somewhat complicated issue, there is no pretense that the matter has been resolved in any definitive way.

Kasha's rule states that molecular fluorescence is from the lowest singlet state, S_1. In extended polymeric systems, one must consider whether or not S_1 is dipole allowed.[20-22] For this requirement to be met, the transition from the lowest singlet to the ground state must be a

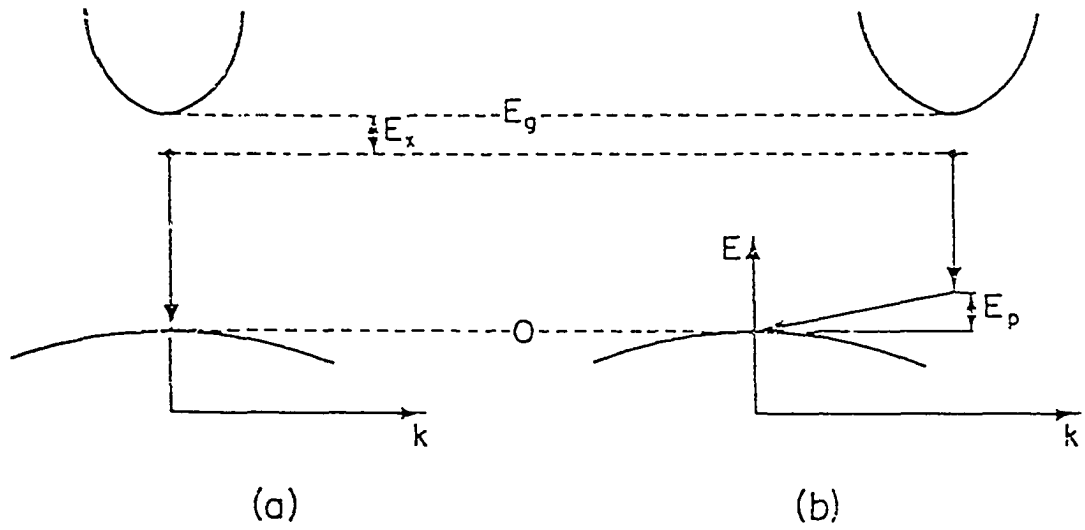

Exciton recombination: (a) direct; (b) indirect.

Figure 11
Direct and indirect exciton recombination processes[18]

transition between states of unlike parity. The ground state in these conjugated polymer systems is symmetric and assigned to the 1^1A_g notation of group theory. Therefore, dipole allowed transitions can only take place from excited, antisymmetric states. Luminescence from π-conjugated polymers has been assigned to transitions from the 1^1B_u singlet state.

There has been much recent work done to understand the nature of the excited state energy levels in conducting polymers.[23-26] These excited states include singlet excitons with odd (B_u) and even (A_g) parity, the continuum band and the triplet manifold.[20,23-24] It has been theorized that the relative locations of the 1^1B_u and the lowest symmetric 2^1A_g singlet exciton levels are most predominantly determined by two parameters: the electron-electron interaction and the alternation parameter (δ) in the π electron transfer integral along the polymer chain.[21] Experimental work focusing on this model will be described later.

Electron Spin Resonance (ESR)

Electron Spin Resonance (ESR) occurs when electronic energy levels are split in a D.C. magnetic field and microwave photons are present for absorption by the spins in the sample. Only when the energy of these photons is equal to the energy difference between these levels will this absorption take place (see Figure 12). We call this coincidence of microwave photon energy and level splitting a magnetic resonance condition. Specifically:

$$g \beta H_o = h \nu$$

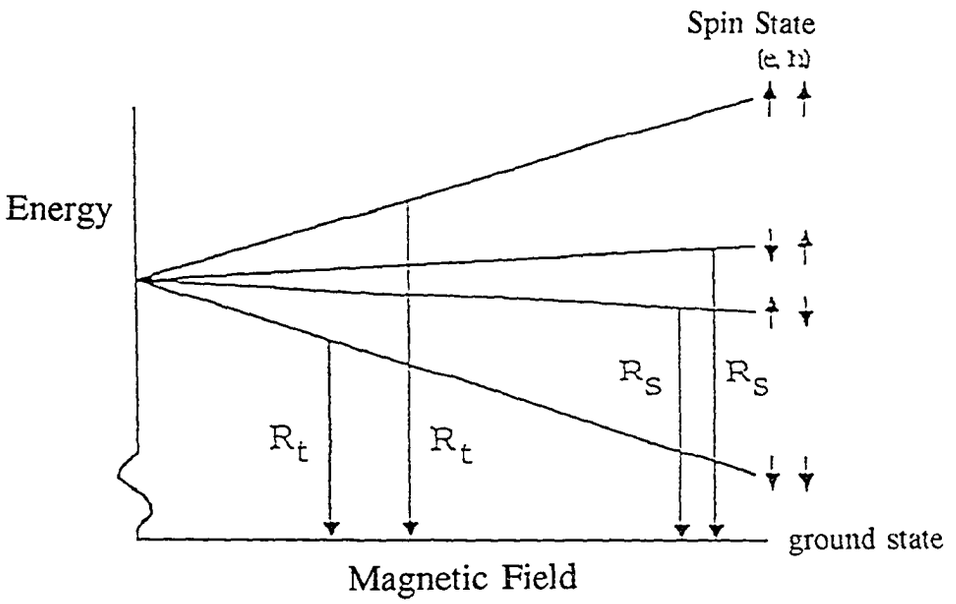

Figure 12
Zeeman level splitting versus
applied D.C. magnetic field

where: **g** is the Lande splitting factor (2.00232 for free electrons),

β is the Bohr magneton (0.927×10^{-20} ergs/gauss),

$\mathbf{H_0}$ is the resonant magnetic field,

h is Planck's constant (6.6262×10^{-27} erg·second),

and ν is the microwave photon frequency

Generally, the microwave photon energy (frequency) is constant while the D.C. magnetic field is swept through the resonant field. Prior to application of microwaves the occupation of the two Zeeman sublevels will obey the Boltzmann distribution. If there are free, or unpaired, spins present in the sample being studied, then absorption will occur and a peak in the absorption spectrum will be observed. The area under the absorption peak will be proportional to the number of unpaired spins and this number can be thus calculated as:

$$\mathbf{AREA = A\ N\ h\ \nu\ /2\ k_B\ T}$$

where: **A** is a constant,

N is the number of free (unpaired) spins,

and $\mathbf{k_B}$ is Boltzmann's constant (1.3807×10^{-16} erg/°K)

In this work, the microwave frequency was approximately 9.3 Gigahertz (X-band) in

all of the experiments. It is possible to hold the D.C. magnetic field constant while scanning the microwave photon frequency about this central value, but it is not desirable. Maintaining constant microwave power, critical coupling of the microwave cavity with the microwave bridge and a reasonable signal-to-noise ratio are factors working against this method.

Besides obtaining a value for the number of free spins in the sample, there are other important quantities which can be deduced from ESR. Some of these include the spin-spin and the spin-lattice relaxation times determined from available linewidths, lineshapes and saturation behavior as well as important structural and dynamical information obtained from the temperature dependence.[27]

Photoluminescence Detected Magnetic Resonance (PLDMR)

In photoluminescence detected magnetic resonance (PLDMR) experiments, the role of the microwave photons is similar to that in ESR. In other words, at resonance, spin carrying species like electrons and polarons can absorb microwave photons and change the orientation of their spins. This can enhance an already dominant spin-dependent process. It can do this, however, only at the expense of another more slowly evolving process. Because there are usually several processes by which spin carrying species can either recombine or become bound with other states present in the material under study, the analysis of PLDMR data is extremely complicated.

Basically, when doing a PLDMR experiment, one measures changes in the

photoluminescence output on-resonance as compared to off-resonance. This can be done if the microwaves are modulated and the PL signal is then fed back to a lock-in amplifier. Then, only changes in the PL brought on by microwave induced changes in charge carriers' spin orientations will be measured as signal.

The most obvious example of a process yielding PLDMR would be the fusion of positive and negative polarons with opposite spin orientations into singlet excitons which decay radiatively. The net result being that the population of polaron pairs with antiparallel spins will be depleted leaving a much larger population of pairs with parallel spins. The resonance condition would yield a net transfer of species with parallel spins into those of antiparallel spins which could then recombine radiatively. There will be an increase in the PL signal and a positive or "enhancing" PLDMR will be recorded. It has been suggested that this picture describes the narrow enhancing PLDMR observed in conjugated polymers at visible laser excitation. If, on the other hand, the most efficient spin-dependent process for recombination in a material is non-radiative, then occupancy of these participating sublevels will be depleted more quickly than, say, a competing radiative one. In this case, at resonance, the nonradiative process will be enhanced since the net transfer would be in favor of the depleted populations of the species which decay nonradiatively. There will be a decrease in the PL signal and a negative or "quenching" PLDMR will be recorded.

Another mechanism by which a PL-enhancing narrow resonance might be observed is the following: Polarons may serve as nonradiative quenching centers for singlets. At resonance, the fusion of polaron pairs to singlets would be enhanced as described above.

They would decay nonradiatively and add nothing to the PL. However, their removal from the system as nonradiative quenching centers for singlets which do decay radiatively would yield a net increase in the PL and thus the PL-enhancing narrow resonance observed in conjugated polymers could be explained by this alternative mechanism. Some of the results to be shown later will be discussed in light of the two competing pictures just described.

It is generally accepted that it is the decay of singlet excitons that yields the PL in π-conjugated polymers. The PLDMR of most materials, if detectable, yields the basic features shown in Figure 13. The central narrow resonance is known as the polaron resonance since it is widely accepted that polarons play a primary role in producing this signal. The broader spectrum that surrounds the central peak is due to triplet excitons. This is a broad powder pattern as it consists of a sum of contributions from all orientations. There is also a triplet signature which is detected at half field and is due to the $\Delta m_s = 2$ transitions among the sublevels of these triplets.

The characteristics of the triplet spectrum of a material are dependent upon parameters contained in the spin Hamiltonian of the triplet state which has the form:[28,29]

$$\mathbf{H} = g\,\beta\,\mathbf{H}\cdot\mathbf{S} + D\,[S_z^2 - S(S+1)/3] + E(S_x^2 - S_y^2)$$

where $D = 3\,g^2\,\beta^2\,\langle(r^2 - 3z^2)/r^5\rangle/4$

$E = -3\,g^2\,\beta^2\,\langle(x^2-y^2)/r^5\rangle/4$

x, y and z are the coordinates of the relative positions of the two spins

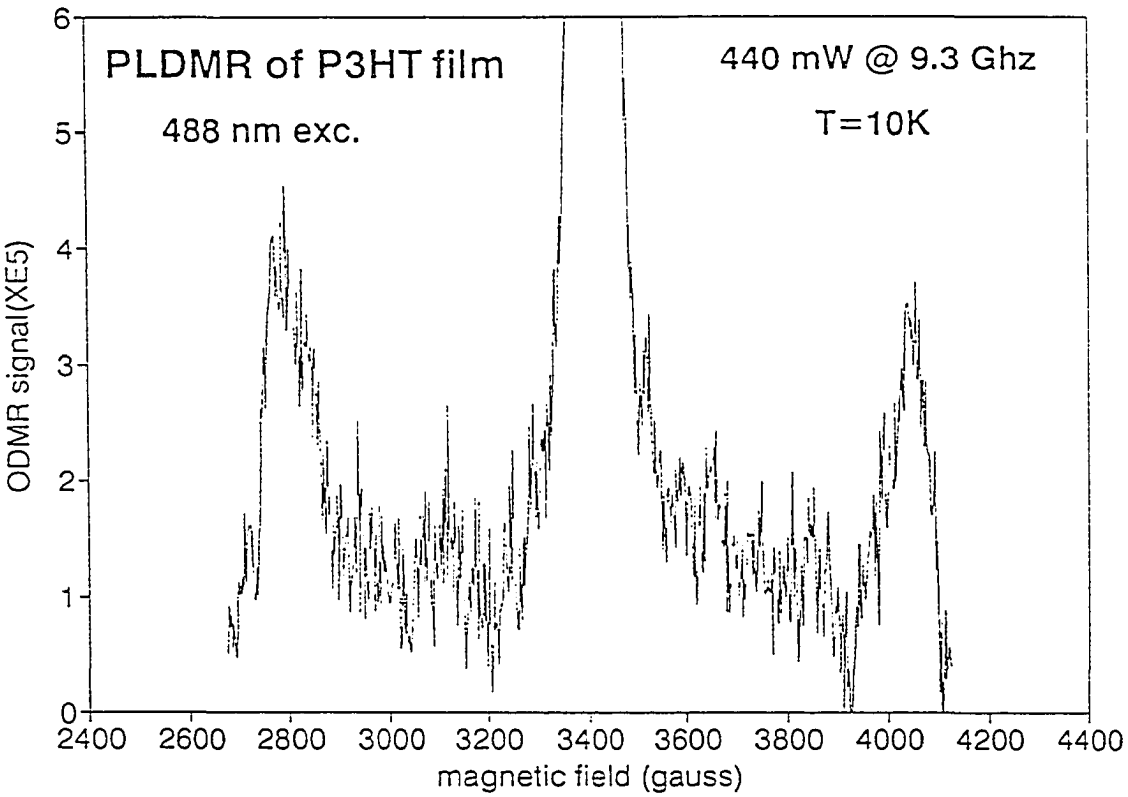

Figure 13
Typical PLDMR spectrum

and the spin-orbit and hyperfine terms have been neglected.

The latter two terms determine the character of the spectrum and **D** and **E** are known as the zero field splitting (ZFS) parameters. If the triplet is quasi two-dimensional so that $\langle 3\,z^2/r^5\rangle$ « $\langle 1/r^3\rangle$, then the value of **D** measures the effective size of the triplet and **E** measures the amount of deviation from axial symmetry that the π electron distribution exhibits.[30]

The X-band PLDMR of π-conjugated polymers, excited at $\lambda_{ex} = 488$ nm, has invariably yielded three resonances: (i) A narrow ($12 \leq \Delta H_{1/2} \leq 20$ gauss) PL-enhancing resonance was attributed to magnetic resonance enhancement of singlet exciton generation by fusion of positive (p^+) and negative (p^-) polarons. (ii) Broad full- and (iii) half-field triplet powder patterns were attributed to similar generation of singlets from triplet-triplet exciton fusion. Other recent studies, however, are providing mounting evidence for the roles of bound p^+-p^- pairs,[31,32] defect stabilized polarons,[33,34] and the various antisymmetric 1^1B_u and 1^3B_u and symmetric m^1A_g and 1^3A_g singlet and triplet excitons, respectively.[23] In particular, it appears that visible photoexcitation of luminescent polymers produces the "rigid" 1^1B_u singlet exciton. In an effort to study higher-gap polymers and search for a distinct ODMR signature of other excitations, possibly electron- and hole-like, we have measured the resonances of various polymers excited at bands around λ_{ex} ~250, 308, 330, 353, 380, 406, and 430 nm, and compared the spectra to those obtained at $\lambda_{ex} = 488$ nm. The polymers included poly(p-phenylenevinylene) (PPV), the dialkyloxy derivatives of PPV, poly(p-phenyleneacetylene) (PPA), and poly(3-alkylthiophenes) (P3ATs).

Upon investigation into the analysis of the PLDMR of the PPVs and P3ATs, an attempt to pinpoint a more precise excitation wavelength where the onset of the PL-quenching resonance (below) appears in these polymers was deemed necessary. It may be the case that the onset of this PL-quenching resonance is brought on by photo-excited, fully separated spin carrying charge species. If this is so, then it is the excitation source energy at which the PL-quenching begins that separates the continuum band from the ground state. A lower bound on the binding energy of the singlet exciton responsible for the bulk photoluminescence can then be calculated if the location of the onset of the absorption (presumably to the ^1B_u singlet exciton state) is known.

The effects of photo-oxidation on the narrow PLDMR of PPV films were investigated. If the intensity of the narrow PLDMR is affected by photo-oxidation, then some conclusions could be drawn about the nature of the mechanism which produces the narrow resonance. It is known that photo-oxidation quenches the PL and that the weaker PL signal is due to fast radiative decay of singlets.[35] Presumably, these singlets decay before they are able to be quenched at the carbonyl centers produced as a result of photo-oxidation as the more slowly decaying ones are. If it is the role of polarons to act as nonradiative quenching centers for singlets, then their effect on the PL-enhancing narrow resonance would be reduced after photo-oxidation. If it is the role of polarons at resonance to fuse more readily to singlets and decay radiatively adding to the overall PL, the PLDMR would seem to remain unaffected by photo-oxidation. A secondary objective in this study is to examine independently the effects of photo-oxidation on the PL-enhancing and PL-quenching resonances and note any important

differences or similarities.

Identical dioctoxy poly(p-phenylenevinylene) (DOOPPV) films were photo-oxidized with incident radiation of λ_{ex} ~353 nm for 0, 10, and 90 seconds. As determined by L. Rothberg and coworkers, the effects of photo-oxidation in conjugated polymers are essentially λ_{ex} -independent. The PLDMR of the narrow polaron resonance in these films was then measured.

Films of unsubstituted PPV and CN-PPV (Figure 3, top) were obtained from Neil Greenham and coworkers of the Cavendish Labs of Cambridge University. As they were of unsubstituted PPV, they were not soluble and we were not able to seal them using the method to be described later into evacuated quartz tubes. The films were kept fresh in a glovebox until needed. Then, the films, in turn, were placed immediately into the cryostat of the PLDMR system and thereafter remained in a helium atmosphere until completion of the work. The purpose for measuring the temperature dependence of the half-field is in connection with similar experiments done on unsubstituted PPV/CN-PPV layered Light Emitting Diodes (LEDs). It seems that the half-field resonance in the ELDMR (Electroluminescence Detected Magnetic Resonance) of these LEDs is clearly seen at high temperatures whereas the triplet resonance in the unsubstituted PPV is attenuated quickly at temperatures far lower than 135 K. Our separate experiments performed on each polymer may tell us which is the emissive layer.

As stated earlier, basic studies of the photo- and device-physics of π-conjugated

polymers have been motivated by rapid advances in the development of polymer based LEDs. Since PPV has successfully provided the emissive layer for reasonably stable and efficient LEDs, the PLDMR of poly(p-di(phenyleneethynylene)phenylenevinylene) (PDPEPV) see Figure 6), with its vinylene unit, has been chosen for study and the details are provided later in this thesis.

The last group of polymers that has been studied in this work are the PPC derivatives. The polymer shown in Figure 5 at the top of the page is interesting as it has similar luminescent and conductive properties to those of polydiethynylsilane (PDES) which have provided some interesting physics.[36] The study of the two remaining polymers of Figure 5 was motivated by the discussion above concerning the underlying nature of photoluminescence.

EXPERIMENTAL PROCEDURE

Sample Preparation

The polymers which were used in this work were obtained from various sources. The PPEA derivatives (see Figure 2), the PDBOPA (see Figure 4, middle) and the polycumulenes and their variants (see Figure 4, bottom and Figure 5) were obtained from Professor Tom Barton's chemistry group at the Ames Laboratory. The P3HT (see Figure 4, top) and P3DT were obtained from Dr. K. Yoshino of the University of Osaka and the PPV derivatives were obtained from Dr. K. Yoshino and Dr. Fred Wudl's group at the University of California in Santa Barbara.

Once receiving the polymer powder, the next step was to dissolve some into solution, normally toluene, though other solvents such as benzene, chloroform and tetrahydrofuran could be used. The sample was then sealed as either a film or a solution in an evacuated quartz tube in order to protect it from oxygen and water in the air. To this end, the solution must be placed in a 4 mm outer diameter glass tube which has been sealed on one end using an oxy-acetylene gas torch (see appendix 1).

Next, the polymer-toluene solution is placed into the glass tube using a fine tipped pipette and the solution is degassed. Degassing is essential if the final product is to be a

sealed solution or a sealed film cast on the inside of the glass tube. The procedure involves filling an open-ended dewar with liquid nitrogen. The sample tube with the solution inside has its open end connected to a vacuum pump. The air above the polymer solution in the tube is carefully and roughly pumped out. The solution is then frozen by lifting the liquid nitrogen (mechanically) until the tube end with the solution in it is completely submerged. After twenty seconds or so, the liquid nitrogen is slowly lowered and the gas bubbles out of the solution. After a small amount comes out, the tube is briefly pumped. Care must be taken not to suck the solution into the pump during this step. The process is repeated until, after freezing, no gas bubbles out. The solution is then "degassed". In order to cast a thin film onto the inner walls of the glass tube, the solution must simply be pumped on until all of the toluene has evaporated (see appendix 1).

ESR and ODMR System

There are several subsystems within the complete arrangement (see Figure 14). Each one must be handled in its own independent way while recognizing its contribution to the whole system. The five subsystems are: The cryogenics (described in detail in appendix 1), the microwave system and D.C. magnetic field, the ultraviolet lamp and the laser, the optics and the electronics including the PC-486 computer.

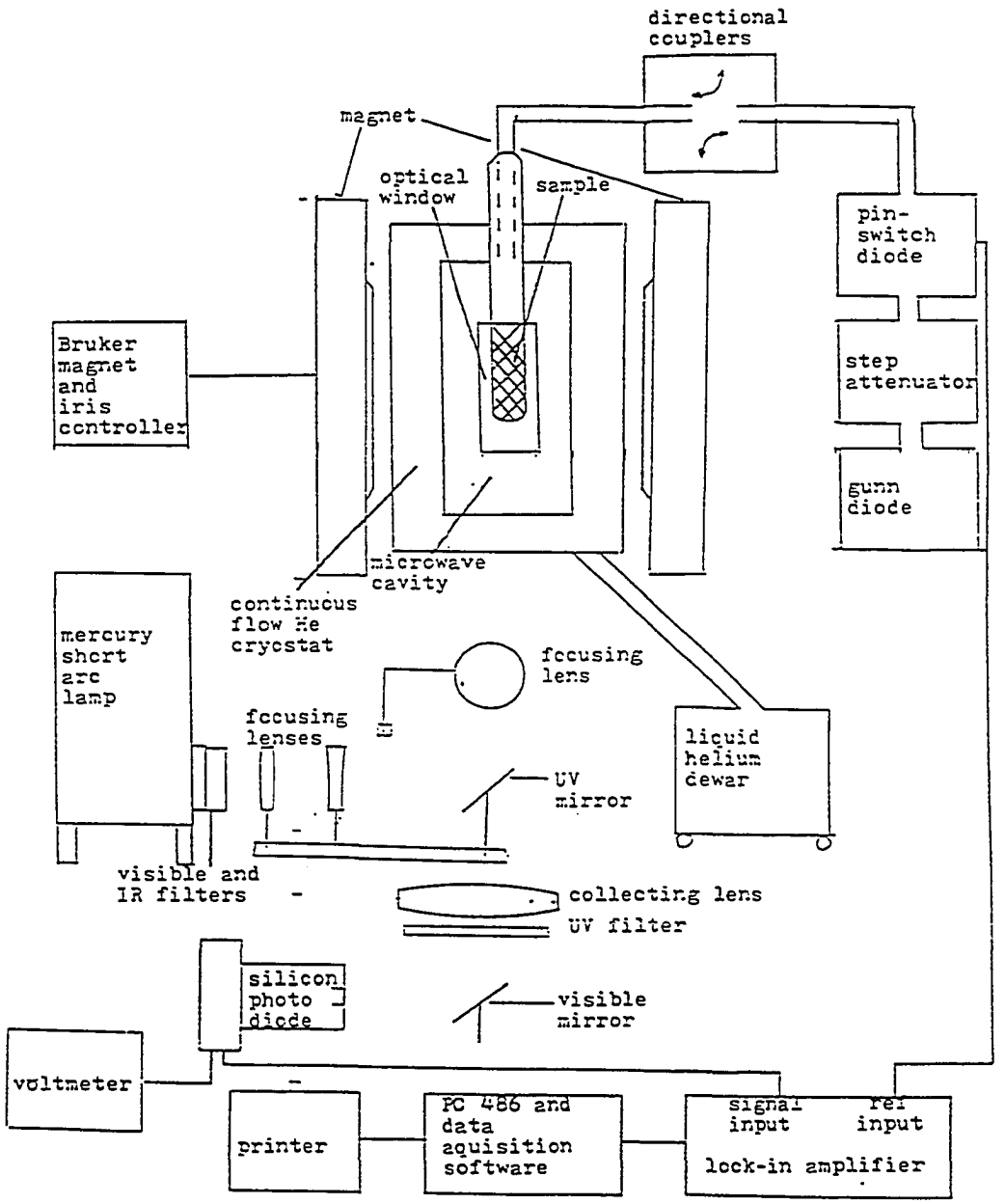

Figure 14
Schematic of laboratory arrangement for
optical and magnetic resonance studies

The Microwaves and the D.C. Magnetic Field

The microwaves for ODMR were generated by a Gunn diode and amplified by a linear amplifier. The power was adjusted using a 0 - 40 db attenuator. The microwaves were then modulated using a pin-switch diode normally chopped at ~330 Hz. The chopped microwaves were then led into the microwave cavity containing the sample. The microwave coupling to the cavity was adjusted for critical coupling and perfect standing waves. A maximum of 1400 mW (0 db attenuation) of microwave power could be fed to the sample. Normally, for samples with average or better signal, 40 mW (15 db attenuation) was used during a PLDMR measurement of the narrow polaron resonance and 440 mW (5 db attenuation) was normally used for full-field powder pattern and half-field measurements.

The Ultraviolet Lamp and the Laser

The sources of incident radiation for the PL and PLDMR measurements were a Hg UV lamp and an Ar^+ laser. The lamp was assembled by the author with the assistance of Mr. P.A. Lane. The Hg bulb emits a broad spectrum of radiation from around 200 nm to the infrared. The lamp was turned on via an igniter switch on the control panel of the power supply. The current was lowered prior to turning the lamp on or off. In order to avoid heating effects, an infrared absorbing filter was placed at the exit port of the lamp housing. Regardless of other filters, this IR filter was always the first that the lamp radiation

encountered. Furthermore, when performing measurements at 250 to 353 nm, a visible light filter was placed on the exit port to reduce the amount of scattered light which would represent itself as noise when reaching the photo-detector. Finally, when performing PL measurements, a third filter to eliminate a narrow band of radiation around 700 nm which escapes the visible and infrared filters was used. When running at wavelengths above 353 nm, the visible filter would be removed but the infrared filter always remained in place. The cooling water was constantly flowing while the lamp was in operation, and not turned off until the lamp was sufficiently cooled down after operation (see appendix 1).

The Optics

The optical arrangement for detection of the PL from samples under illumination by the ultraviolet lamp can be roughly seen in Figure 14. After bouncing off of the mirror contained within the lamp housing itself, the light exits the lamp and encounters the filters mentioned in section C above. When the desired wavelength is 330, 380, 406, or 430 nm, then the appropriate narrow band pass filter must be attached along with the infrared filter to the outside of the exit port of the lamp housing. An arrangement of two fused silica lenses contained the "beam" for later reflection from the broad band reflector. When the desired wavelength was 250, 308, or 353 nm, then the visible and infrared filters were used and the appropriately blazed reflector was inserted into the holder where the broad band pass filter would otherwise be placed. The intensity of light which hits the sample was far greater when

using the blazed reflectors than when using the filters and the broad band pass reflectors. The light from the reflector was then focused with a third fused silica lens onto the sample.

The PL emitted by the sample was focused by a condensing lens at the cavity and onto the lower mirror of a periscope arrangement. This arrangement was necessary because the light from the lamp was lower than the optical table and needed to be brought up. After the PL was reflected from both of the periscope's mirrors, it was directed into a collecting lens that focused it down either into the monochromator for photoluminescence measurements or onto a mirror which then reflected the light directly into the silicon photodiode detector. Low (energy) pass UV filters were inserted before the monochromator/mirror and on the entrance slit to the monochromator/silicon photodiode detector to block out stray light coming from the UV lamp.

The optical arrangement of the system for use with visible laser excitation was simpler. The laser **beam** went through the stabilizer, was redirected using two visible light reflectors and impinged the sample while losing little of its incident intensity along the optical path. The PL was then incident upon and focused by the collecting lens without the need for the periscope arrangement. Low (energy) pass filters cutting in at around 510 nm were used to block out noise from the laser line. The rest was similar to the case for the UV lamp.

The Electronics and the Computer Assisted Data Analysis

The PL signal produced by the photodetector was amplified by a pre-amplifier and then fed into the lock-in amplifier. A lock-in amplifier operates on square wave modulated signals. In an ODMR experiment, it is the microwaves which are "chopped". In measuring a PL spectrum, it is the incident light which is chopped. In experimental practice, there are many other uses besides these where a lock-in amplifier can be valuable, but in every case, one of the quantities which is responsible for producing the signal representing the desired quantity under study must be modulated.

In these experiments, the modulation frequency was fed into the reference input of the lock-in. The actual signal was then matched by the lock-in to the reference. Only that part of the signal input which had the frequency of the reference was read as output by the lock-in and all other sources were filtered out. For example, in the PLDMR experiments, the entire PL was picked up by the photodetector and fed into the lock-in. However, only changes in the PL induced by the chopped microwaves were passed and amplified by the lock-in. The lock-in then turned out to be invaluable in this measurement as the microwave induced changes only accounted for fractional changes of the order of 10^{-7} to 10^{-3} of the entire photoluminescence signal delivered into the signal input.

Once the reference and signal were delivered to the lock-in, these two components needed to be matched for phase. This adjustment was made by adjusting the phase control until either the maximum signal was read, the minimum signal was read and the phase was

then moved off by 90° or, if the signal was two weak to determine, previous experience or trial and error was called upon.

The lock-in had an amplification circuit which was adjusted to match the intensity of the signal it was reading. Signal gains up to 5×10^6 were used with the lock-in available in these experiments. Another adjustment was the time constant. This setting determined how long the lock-in sampled the signal between measurements. A longer time constant would yield less noise but at the cost of resolution. Signal offset could be used if the desired "zero" of the signal output was not consistent with the zero signal output of the lock-in.

The output signal from the lock-in amplifier was fed to the PC-486 computer and read by data acquisition software. In magnetic resonance experiments, the D.C. magnetic field was swept by a sweep controller in tandem with the field controlling console's own center field offset mechanism. That is, both the center field of the magnet and the sweep width were set on the console, then the sweep controller manipulated the sweep. The computer entered value determined the maximum number of sweeps that would be performed, but the experiment would be halted ahead of time if the desired data had been signal averaged to a satisfactory signal-to-noise ratio. It was ultimately important that the sweep width and center field entered into the data acquisition portion of the computer matched those set on the console of the magnetic field controller.

EXPERIMENTAL RESULTS

PL, ESR and UV-excited PLDMR of Poly(*p* - phenyleneethynyleneaniline) (PPEA) Derivatives

Figure 2 shows the structure of the PPEA-type polymers studied in this work. The results of the molecular weight, optical absorption and fluorescence measurements are summarized in Table I. As clearly seen, the peak emission $\lambda_{e,max}$ of the efficient PL is in the blue region of the visible spectrum. However, the onset of the absorption $\lambda_{a,o}$ is in the violet region, and the peak absorption $\lambda_{a,max}$ is in the near UV. Figure 15 shows the PL spectra, excited at ~353 nm. The striking observation is that while the emission of all the films is structureless, the PPDEA solution exhibits some structure and in the spectrum of the PDPEA solution, it is pronounced.

The ESR of the undoped and iodine-doped PPEA are shown in Figure 16. The undoped spectrum suggests an upper limit of ~10^{-9} spins per repeat unit. Upon exposure to iodine vapor, the spin density increased to a value of ~3 x 10^{-6} per repeat unit. The derivative peak-to-peak ESR linewidth was a relatively wide 14 gauss.

The narrow total PL-detected polaron resonance of PDPEA films excited at ~353, ~308, and ~250 nm at 10 K is shown in Figure 17. As clearly seen, the resonance is λ_{ex}-independent, similar to the behavior of PPAs but in contrast to the UV-ODMR of poly(3-alkylthiophenes) (P3ATs) and poly(*p*-phenylenevinylenes) (PPVs) described in a later chapter

Table I. *The weight-average molecular weight M_w, polydispersivity (P.D.), and onset of optical absorption ($\lambda_{a,\rho}$), peak absorption ($\lambda_{a,max}$), and peak emission ($\lambda_{e,max}$) wavelengths (in nm) of the solutions and films studied in this work (see Fig. 1).*

polymer	M_w	*P.D.*	*state*	$\lambda_{a,\rho}$	$\lambda_{a,max}$	$\lambda_{e,max}$
PPEA	$5x10^4$	1.5	solution	430?	389	550
			film	430?	390	550
PPDEA	$7x10^4$	1.4	solution	450?	399	590
			film	450?	417	650
PDPEA	$6x10^4$	2.4	solution	465?	415	520
			film	465?	415	590

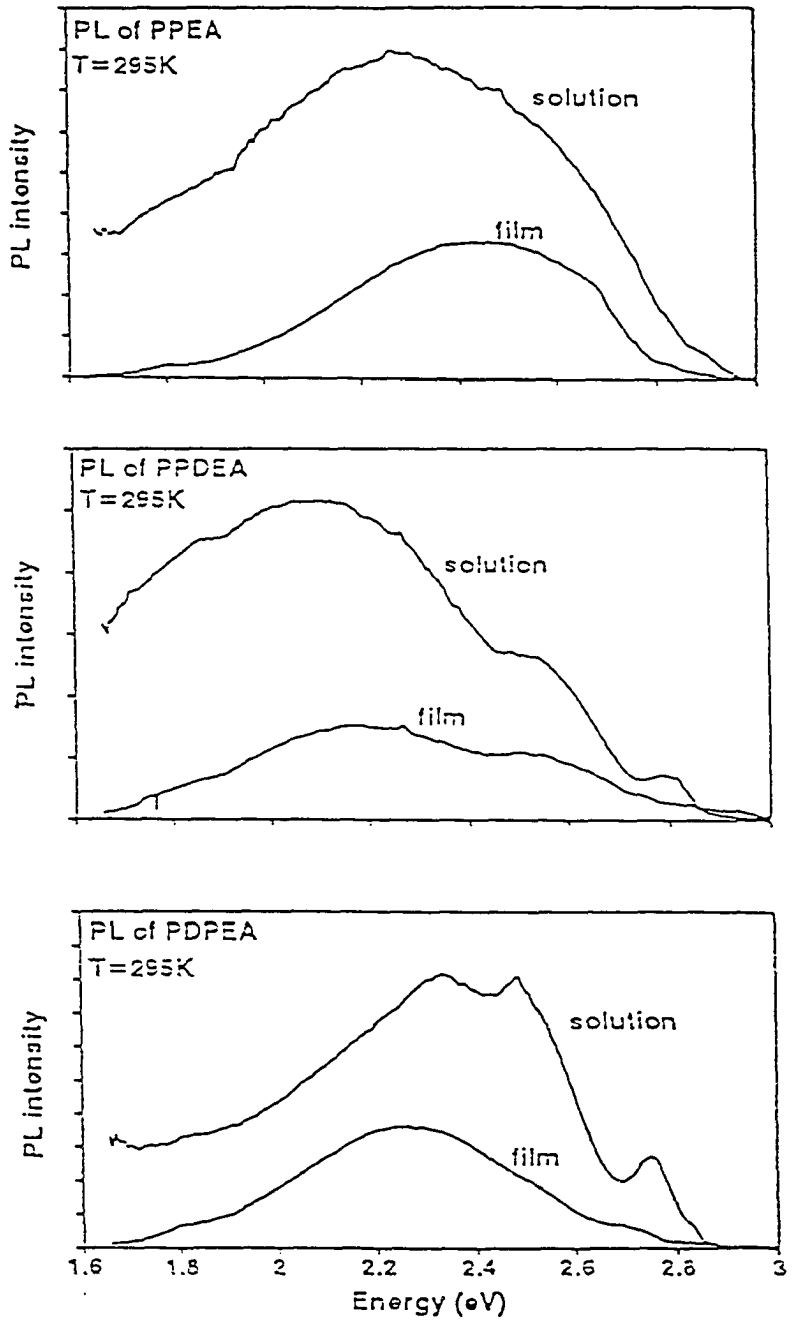

Figure 15
Photoluminescence of PPEA

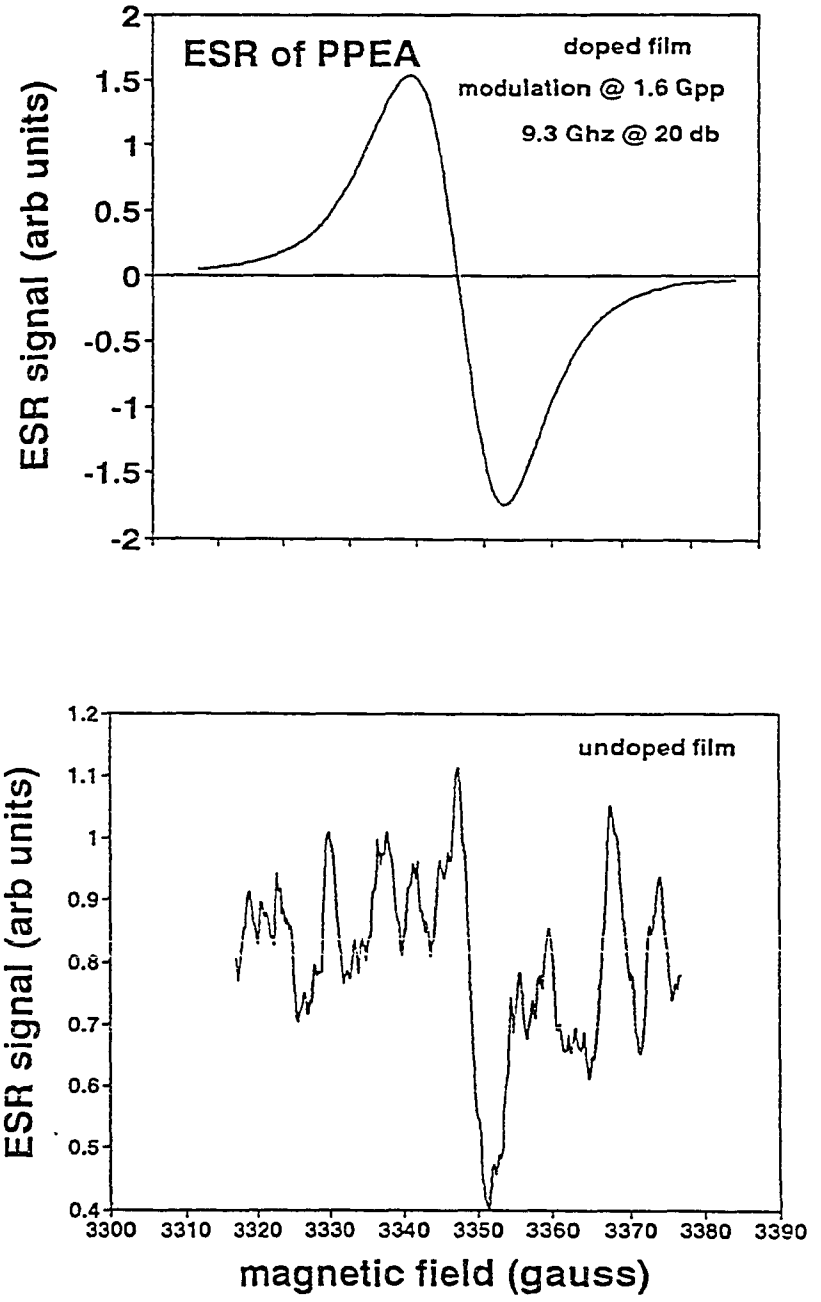

Figure 16
ESR of undoped and
Iodine doped PPEA

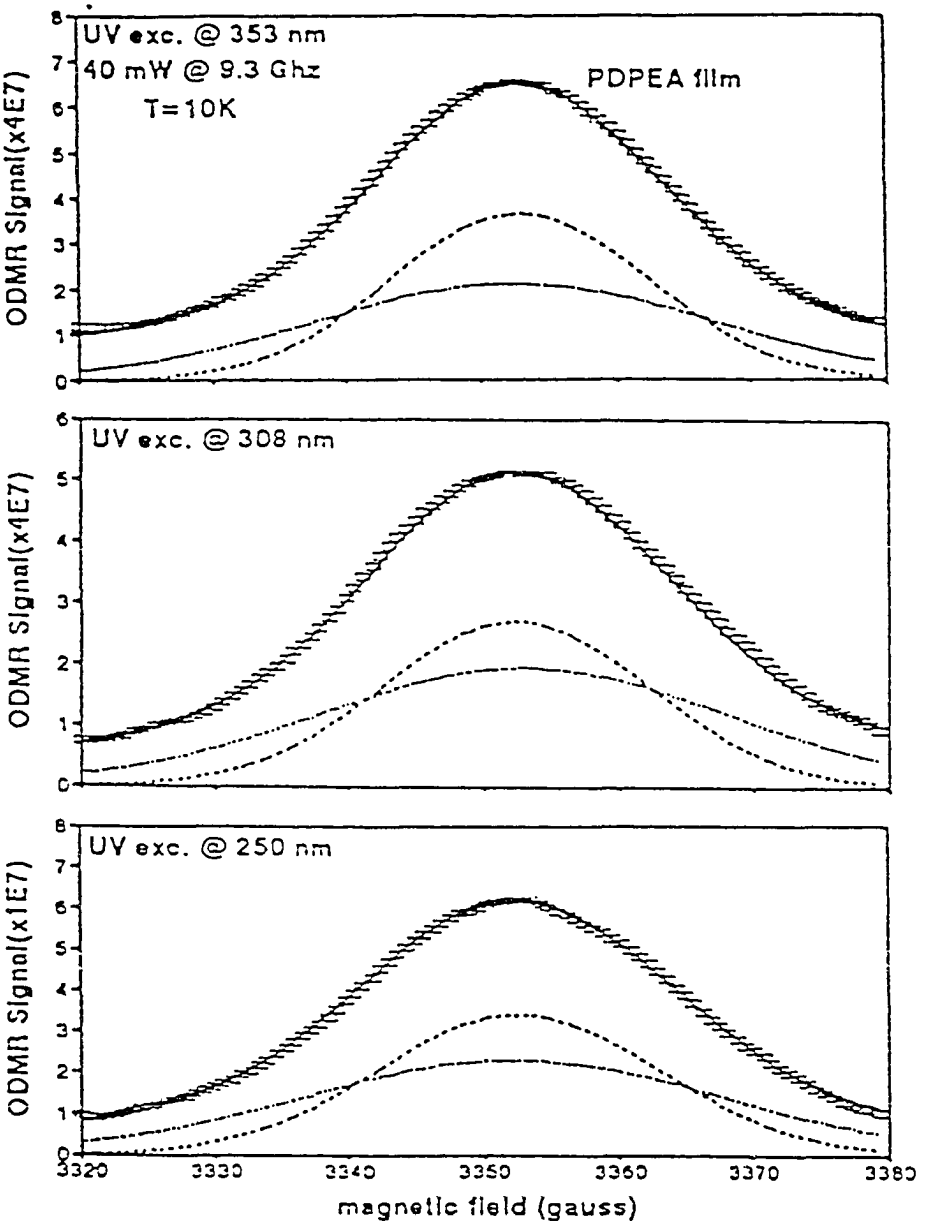

Figure 17
Narrow polaron resonance
of PPEA film

of this thesis. In addition, the full width at half maximum is ~30 gauss, as compared to 10 - 15 gauss in P3ATs[37] and PPVs[38].

The full-field triplet exciton powder pattern resonance of PPEA and PDPEA at λ_{ex} ~ 353 and 250 nm is shown in Figure 18, and the half-field resonance in the latter, at λ_{ex} ~ 353 and 308 nm, is shown in Figure 19. Several observations are noteworthy. (1) The full-field powder patterns are 1200 - 1500 gauss wide, i.e., much broader than those of P3ATs[37] and PPVs[38], and even broader than those of PPAs.[39] (2) In PDPEA, the half-field resonance excited at ~353 nm suggests that two distinct triplet excitons affect the dynamics of the luminescent singlet excitons. (3) Excitation at ~ 308 nm then apparently generates a drastically lower population of the narrower, less localized higher field exciton. (4) Finally, excitation at ~ 250 nm apparently yields a very low density of triplet excitons which affect the PL. This latter observation is similar to UV-ODMR measurements on P3ATs and PPVs described below.

UV-Excited PLDMR Study of PPV, PPA and P3HT

Figures 20-22 display the X-band narrow total PLDMR of DHOPPV, P3HT and 2,5-dibutoxy PPA (DBOPPA) films, respectively, excited at the noted wavelengths at 15 K. The solid lines are the sums of the Gaussian components shown as dotted lines. The PL-enhancing polaron resonance obtained by visible excitation has been extensively described and discussed.[7-9,37-41] The agreement between the observed lineshape and the sums of the

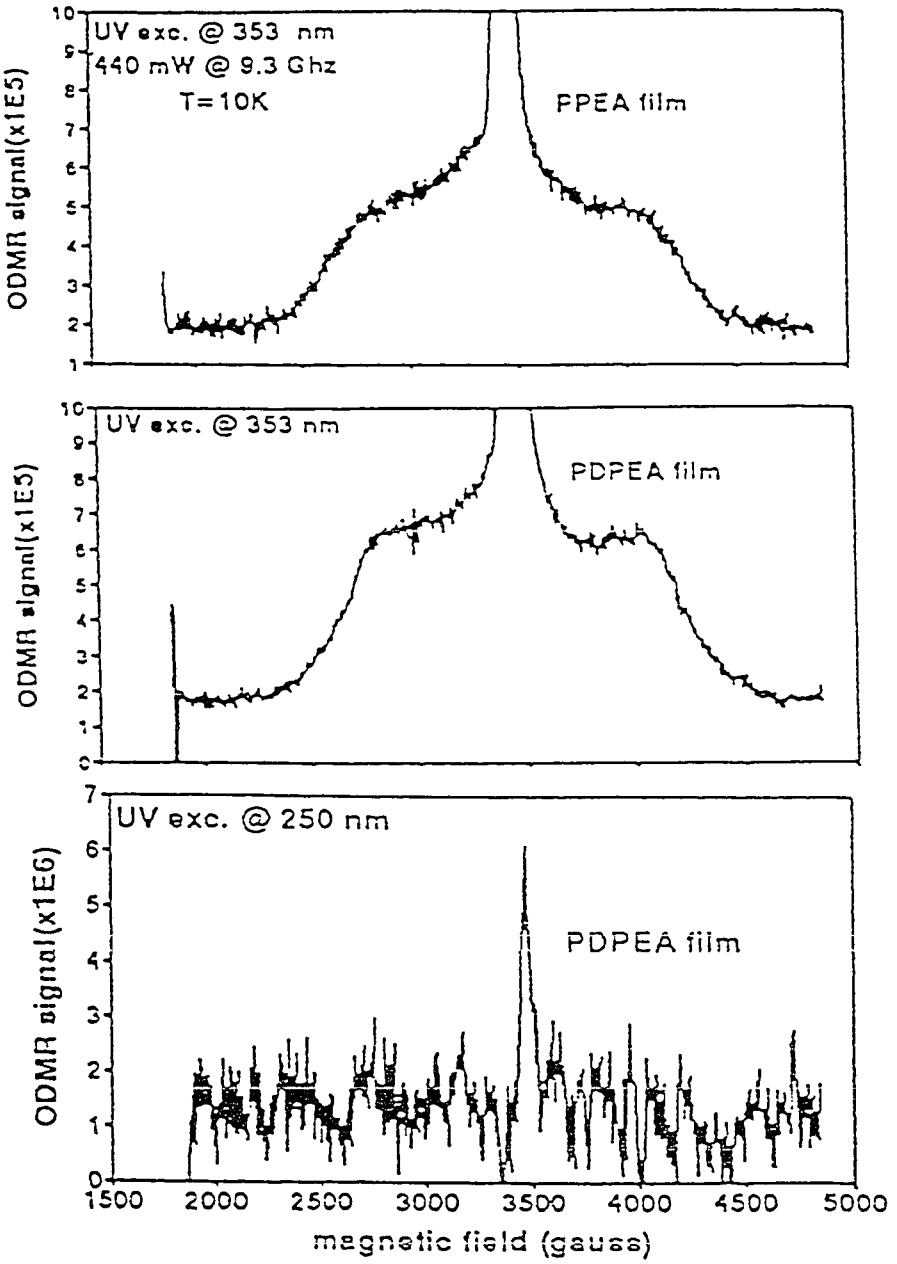

Figure 18
Full-field triplet powder
pattern resonance of PPEA film

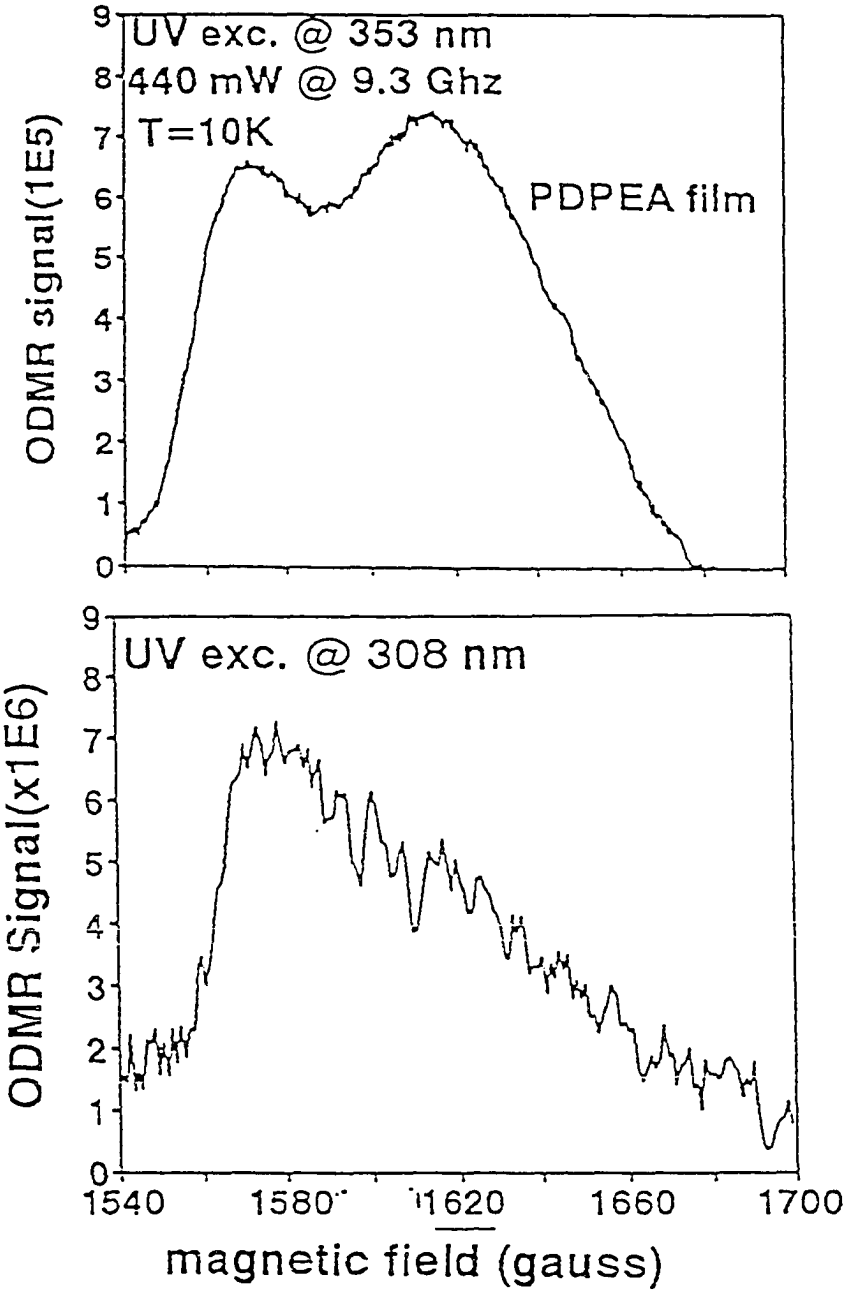

Figure 19
Half-field resonance of
PPEA film

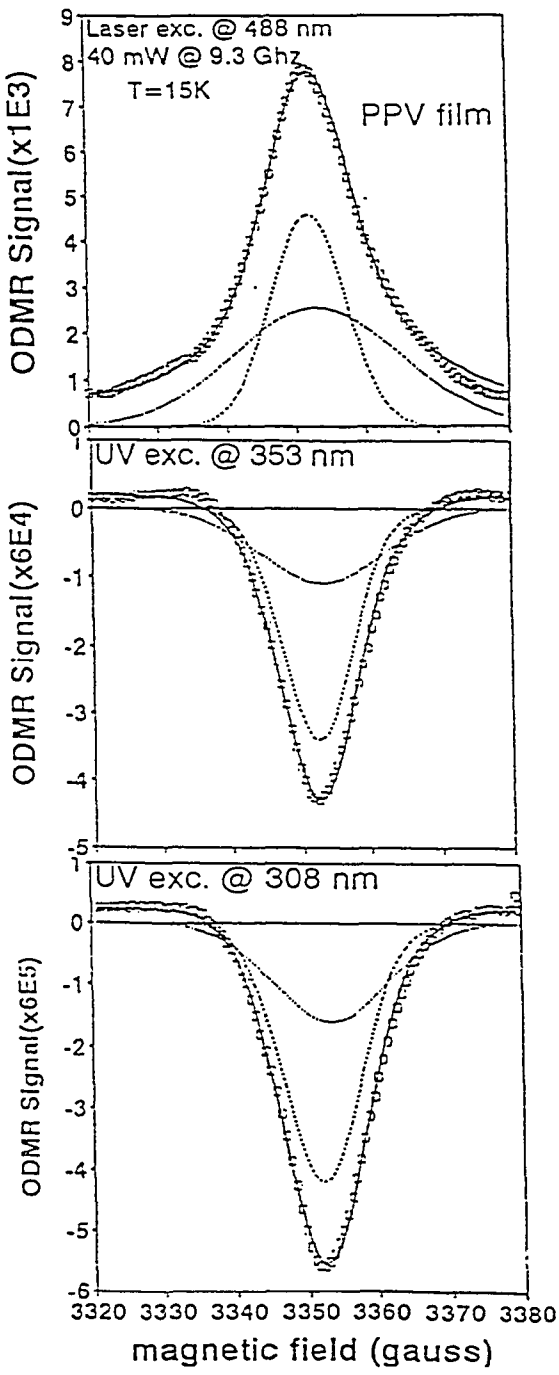

Figure 20
λ_{ex} -dependence of narrow polaron resonance in DHOPPV film

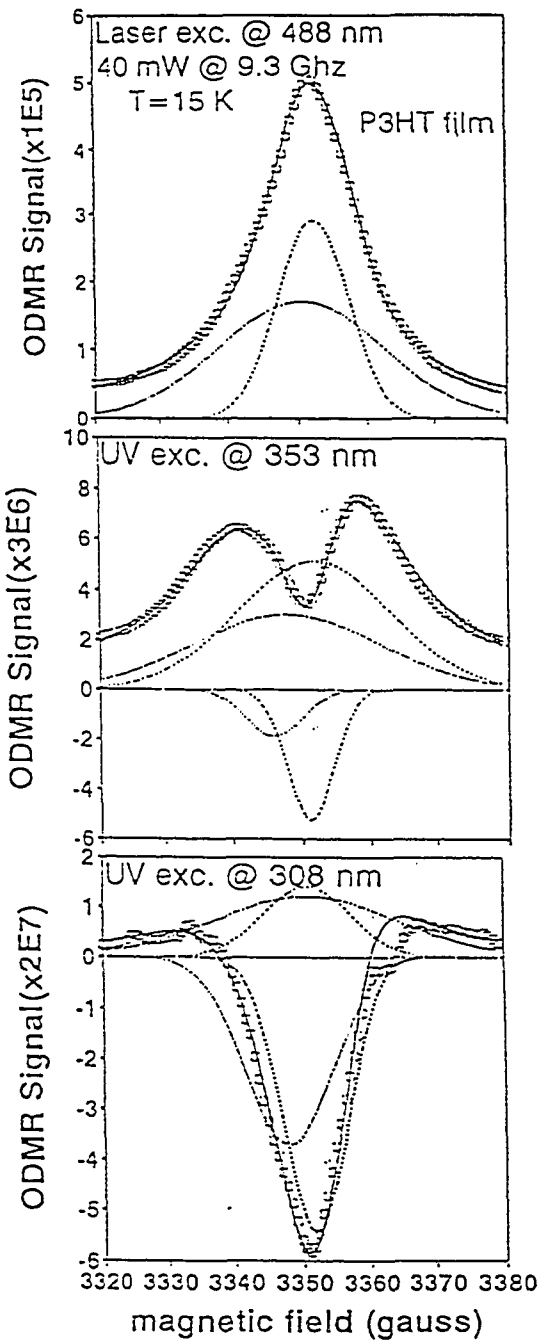

Figure 21
λ_{ex} -dependence of the narrow polaron resonance in P3HT film

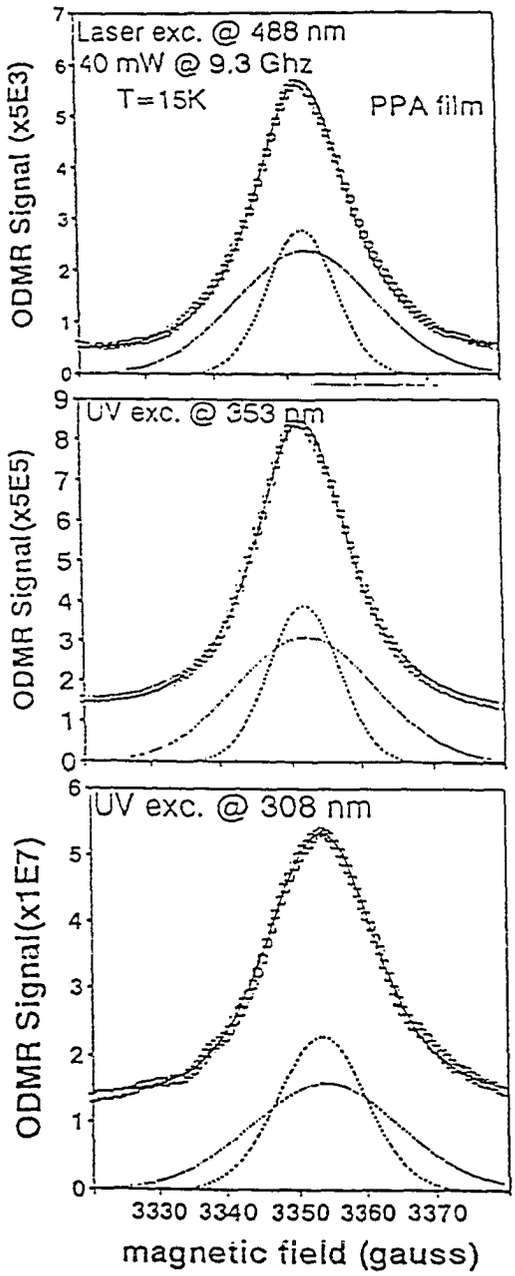

Figure 22
λ_{ex} -dependence of the narrow polaron resonance in PPA films

Gaussian components is clearly excellent in all of these cases. The PL-quenching resonances at λ_{ex} ~ 353 and 308 nm in DHOPPV (Figure 20), the presence of both enhancing and quenching components in P3HT (Figure 21), and the absence of a quenching resonance in PPA (Figure 22) are obviously the most striking results.

Figures 23(a) - 23(e) display the full-field triplet exciton PLDMR of P3HT films at λ_{ex} ~ 308 nm, PPV films at λ_{ex} ~ 353 nm, polyethylene blends of DHOPPV at λ_{ex} ~ 353 nm, and DHOPPV film at λ_{ex} ~ 308 and 350 nm, respectively. Several observations are noteworthy: (i) The λ_{ex}-dependence of the intensities of the narrow PL-enhancing, the narrow PL-quenching, and the triplet exciton powder pattern PLDMR are all different from each other. (ii) The triplet exciton pattern weakens with decreasing λ_{ex}. Thus, in P3HT it is very weak at λ_{ex} ~353 nm and undetectable at $\lambda_{ex} \leq$ 308 nm; in PPV, it is still detectable, but barely, at λ_{ex} ~ 250 nm. (iii) The shapes of the triplet patterns in PPV at λ_{ex} ~353 nm (Fig. 23(b)) and in DHOPPV (Fig. 23(d) and 23(e)) indicate that the triplets are nearly axially symmetric (the zero field splitting parameter $E \approx 0$).

The P3ATs show a quenching resonance at 406 nm (Figure 24). They do not yield any signature of a PL-quenching resonance at 430 nm (see Figure 25). This indicates that the onset of the PL-quenching resonance for these polymer types is within the range between $406 \leq \lambda_{ex} \leq 430$ nm ($2.88 \leq E_{ex} \leq 3.05$ eV).

The DOOPPV and DHOPPV films show a quenching resonance at 406 nm also (see Figure 26). However, though the DOOPPV shows no PL-quenching feature at 430 nm, the DHOPPV does exhibit a quenching resonance (see Figure 27). Upon laser excitation at

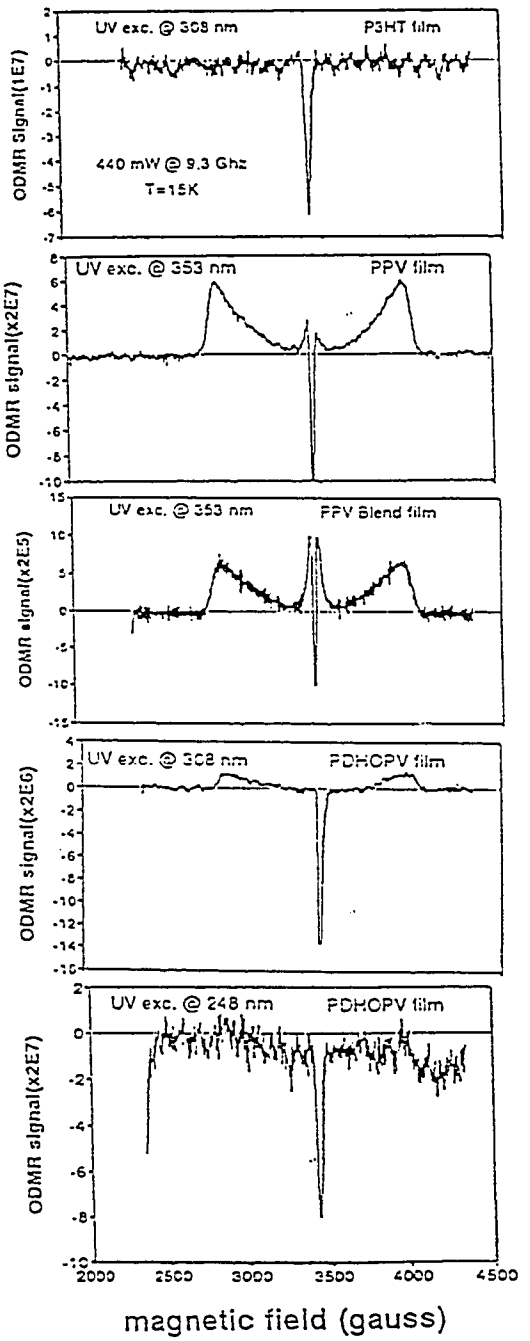

Figure 23
Full-field triplet exciton resonances of P3HT, DHOPPV blends and DHOPPV films

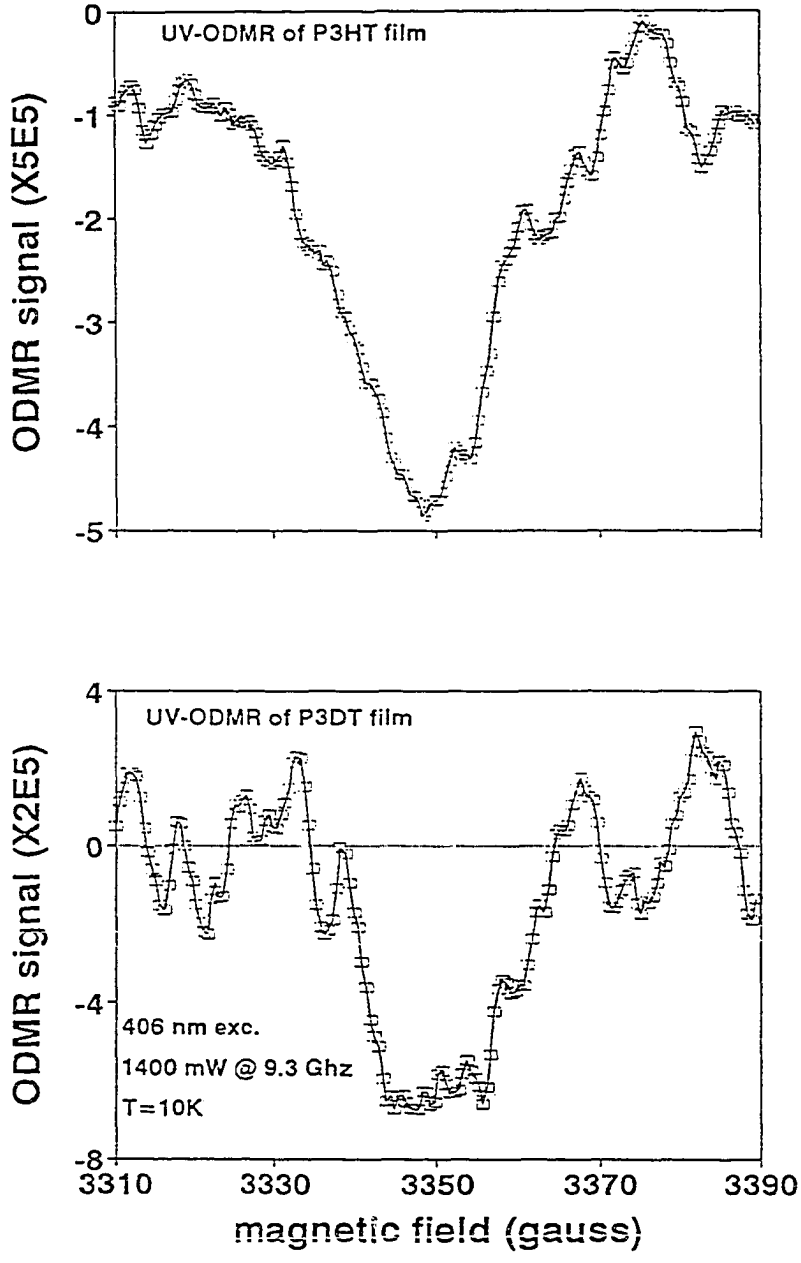

Figure 24
Narrow polaron resonance of
P3HT and P3DT at λ_{ex} ~ 406 nm

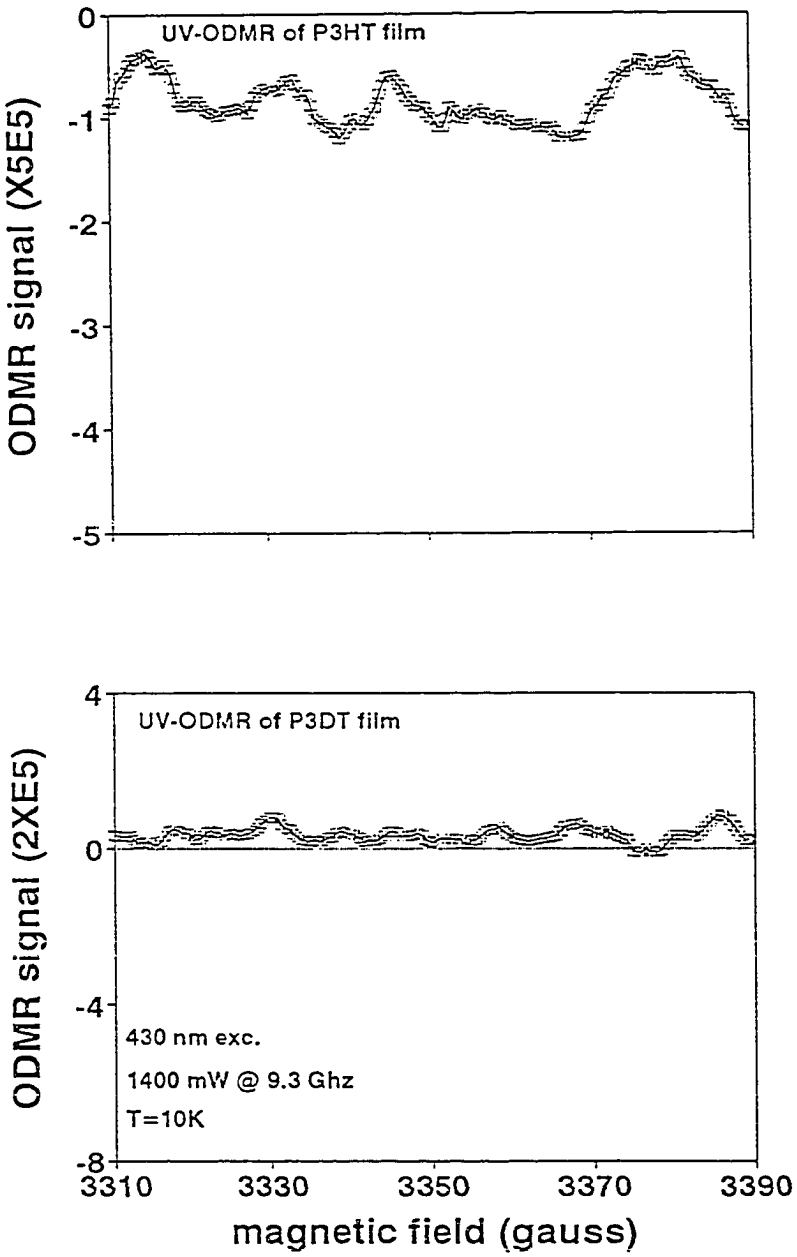

Figure 25
Narrow polaron resonance of
P3HT and P3DT at λ_{ex} ~430 nm

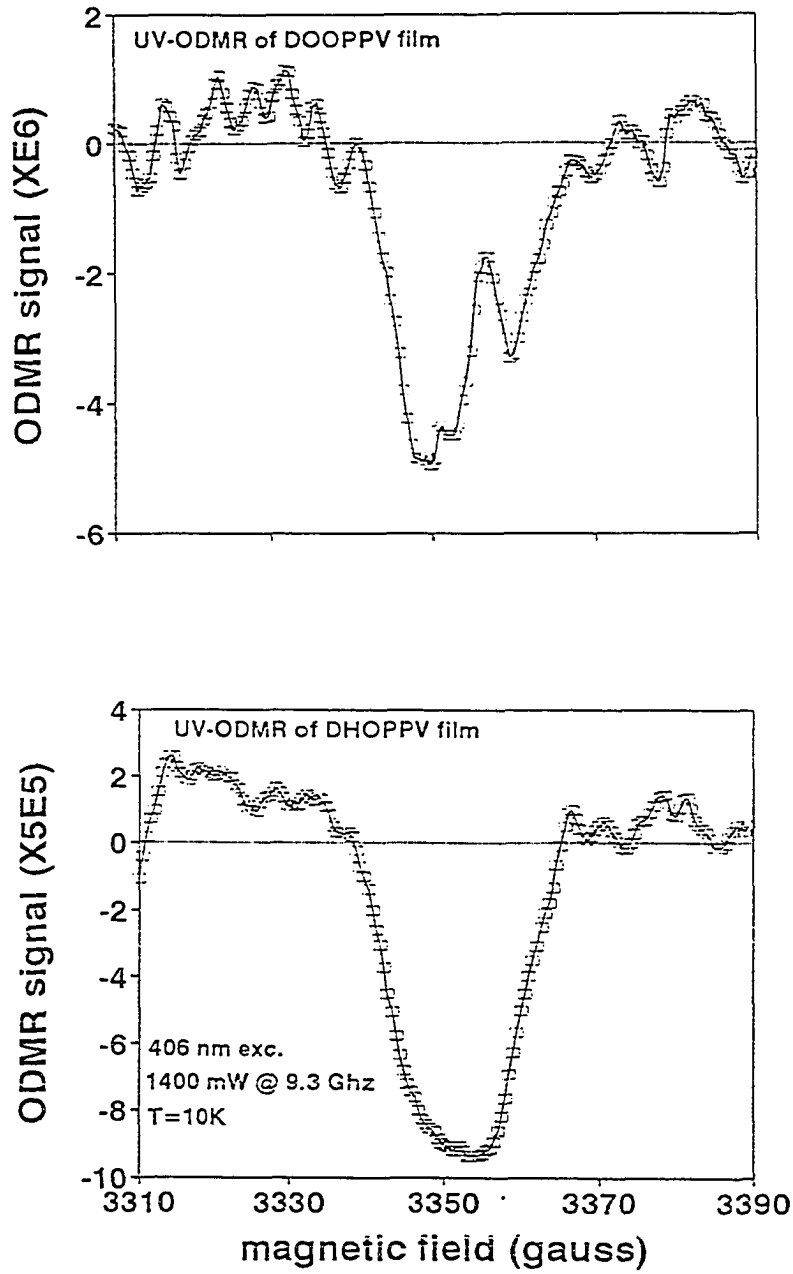

Figure 26
Narrow polaron resonance of DOOPPV
and DHOPPV at λ_{ex} ~406 nm

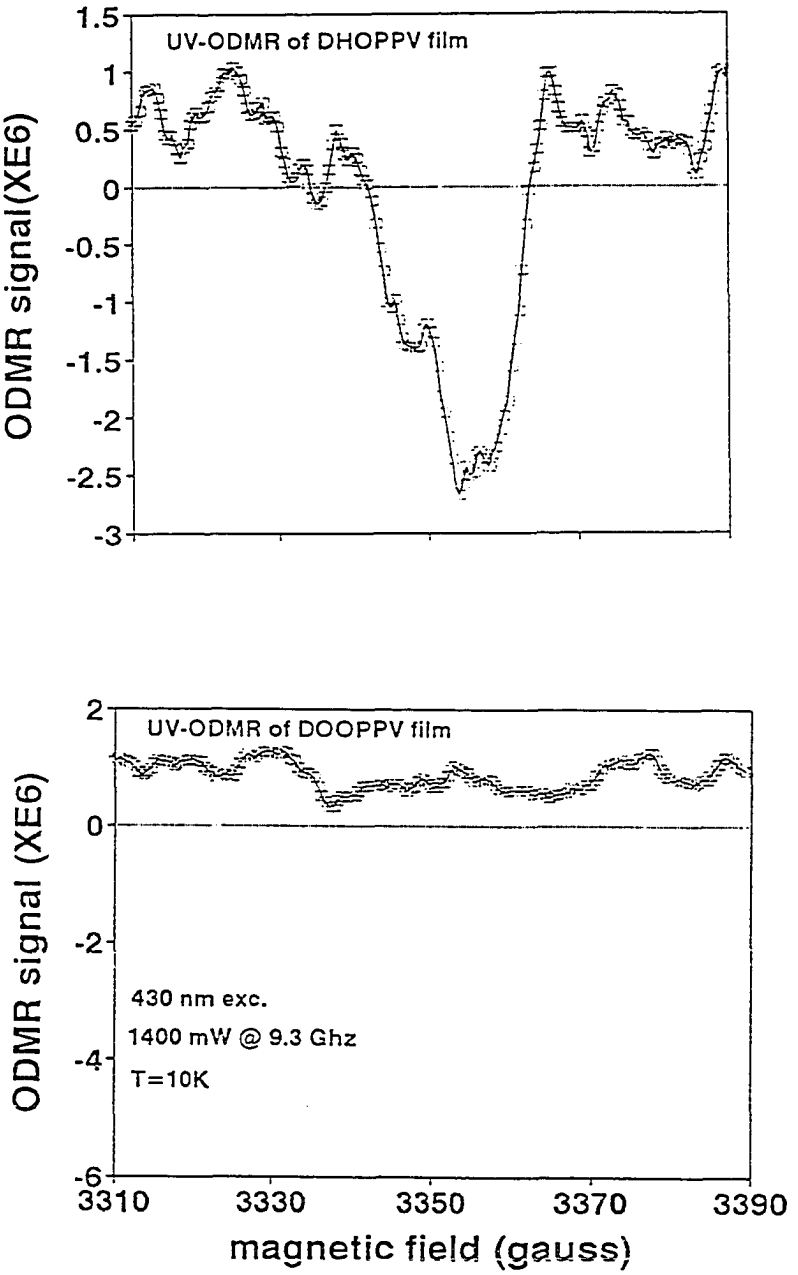

Figure 27
Narrow polaron resonance of DHOPPV
and DOOPPV at λ_{ex} ~430 nm

λ_{ex} = 458 nm, all of the above mentioned polymers do not show any PL-quenching features and do exhibit PL-enhancing narrow polaron resonances (see Figure 28). Therefore, the onset of the PL-quenching resonance in DOOPPV is in the excitation wavelength range $406 \leq \lambda_{ex} \leq 430$ nm corresponding to excitation source energies between 2.88 and 3.05 eV. The onset of the PL-quenching narrow polaron resonance in DHOPPV is between the excitation source wavelengths $430 \leq \lambda_{ex} \leq 458$ nm corresponding to excitation source energies between $2.71 \leq E_{ex} \leq 2.88$ eV.

Though all of the polymers in this study show a clear PL-enhancing resonance at λ_{ex} = 458 nm, it is not clear at the lower wavelengths of 430 nm and 406 nm. This is because the signal-to-noise ratio is much lower at these intermediate wavelengths. Thus, if there is a PL-enhancing characteristic in any of these polymers using these excitation source energies, the attempt to resolve it from the noise has not been successful. It should be noted, however, that at λ_{ex} ~353 nm, some PL-enhancing does appear in the P3HT and PPV blend films (see Figures 21 and 23).

Effects of Photo-oxidation on the UV- and Laser Excited PLDMR of DOOPPV Films

As can be seen in Figure 29, the PL-enhancing narrow resonance at λ_{ex} = 488 nm of the DOOPPV film is clear in unoxidized samples. However, upon photo-oxidation, the PL-enhancing resonance disappears. In contrast, Figure 30 shows that the PL-quenching

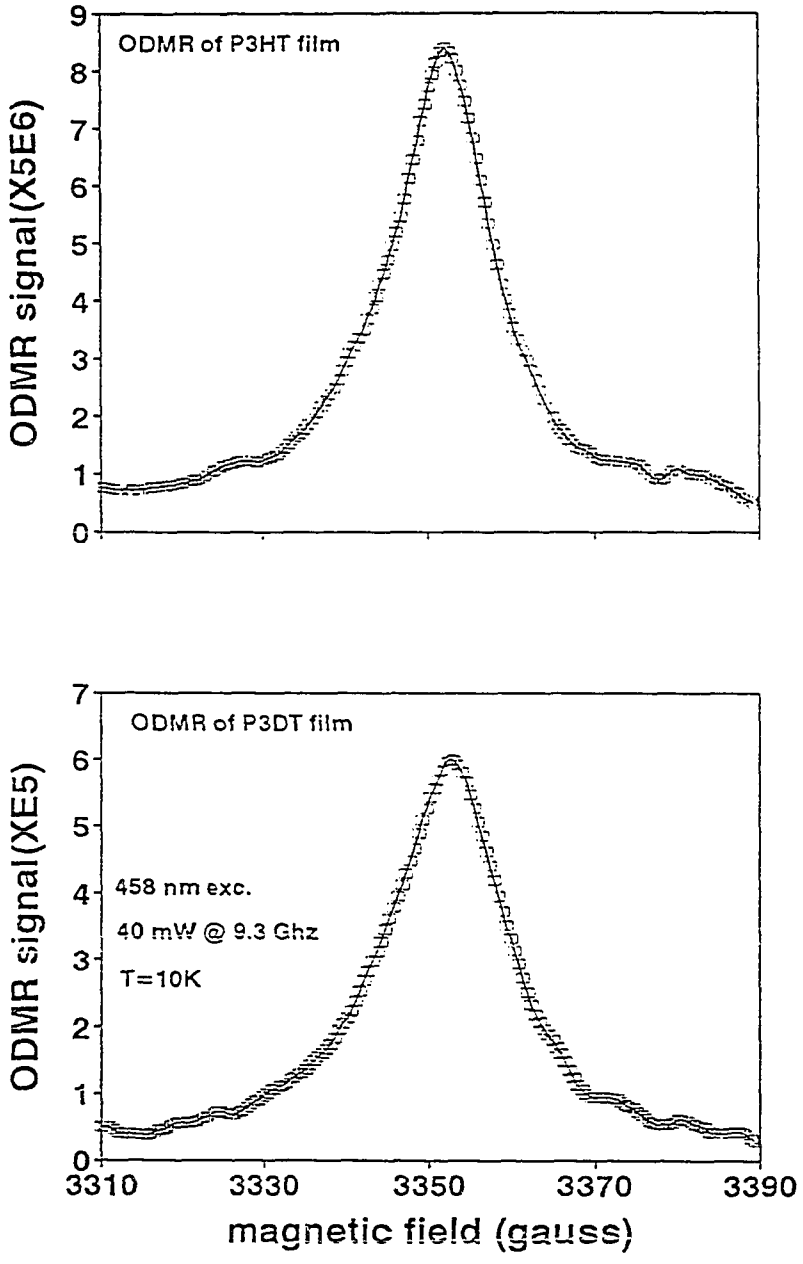

Figure 28
Narrow polaron resonances of (a) P3ATs
and (b) PPVs at $\lambda_{ex} = 458$ nm

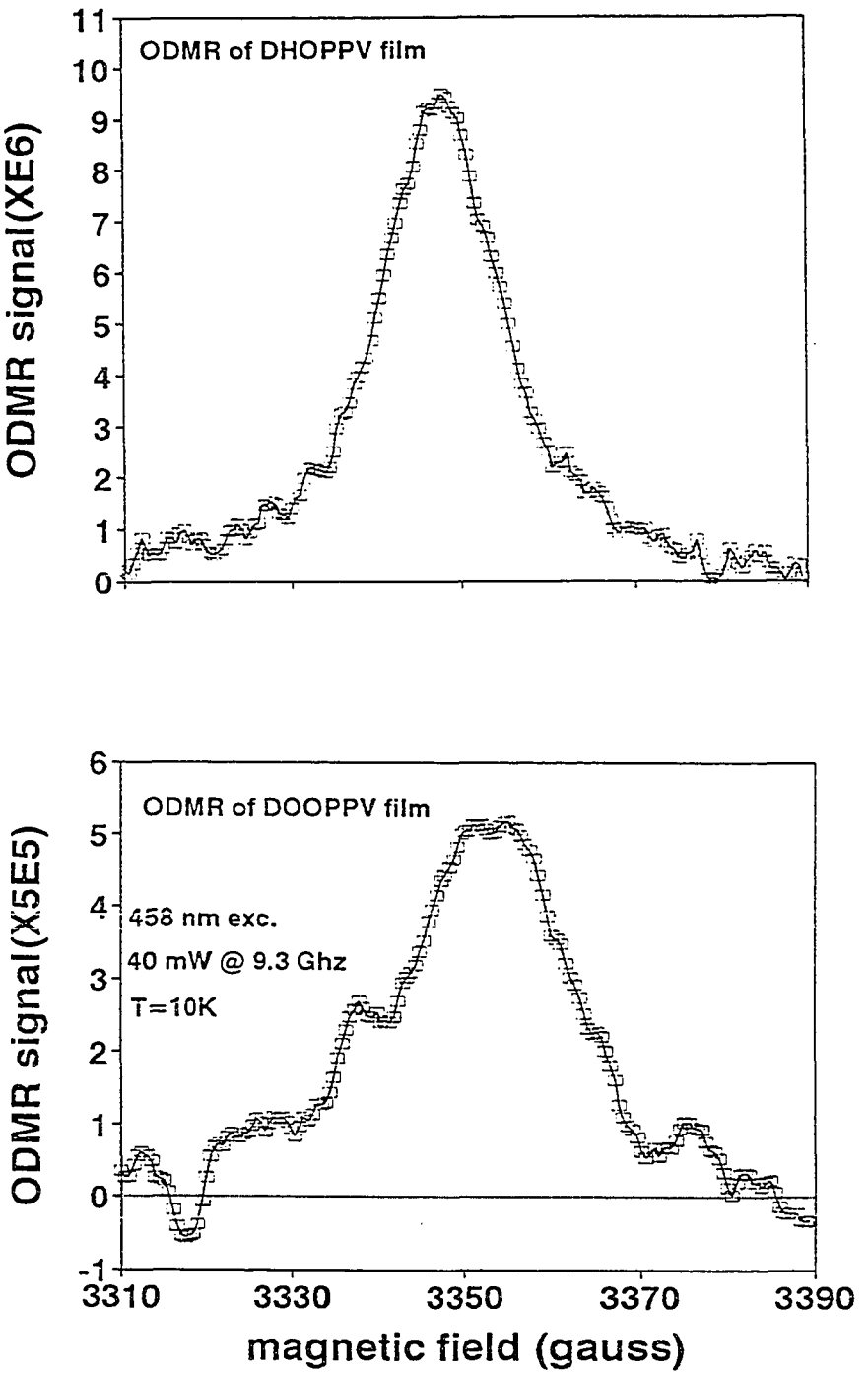

Figure 28 (continued)

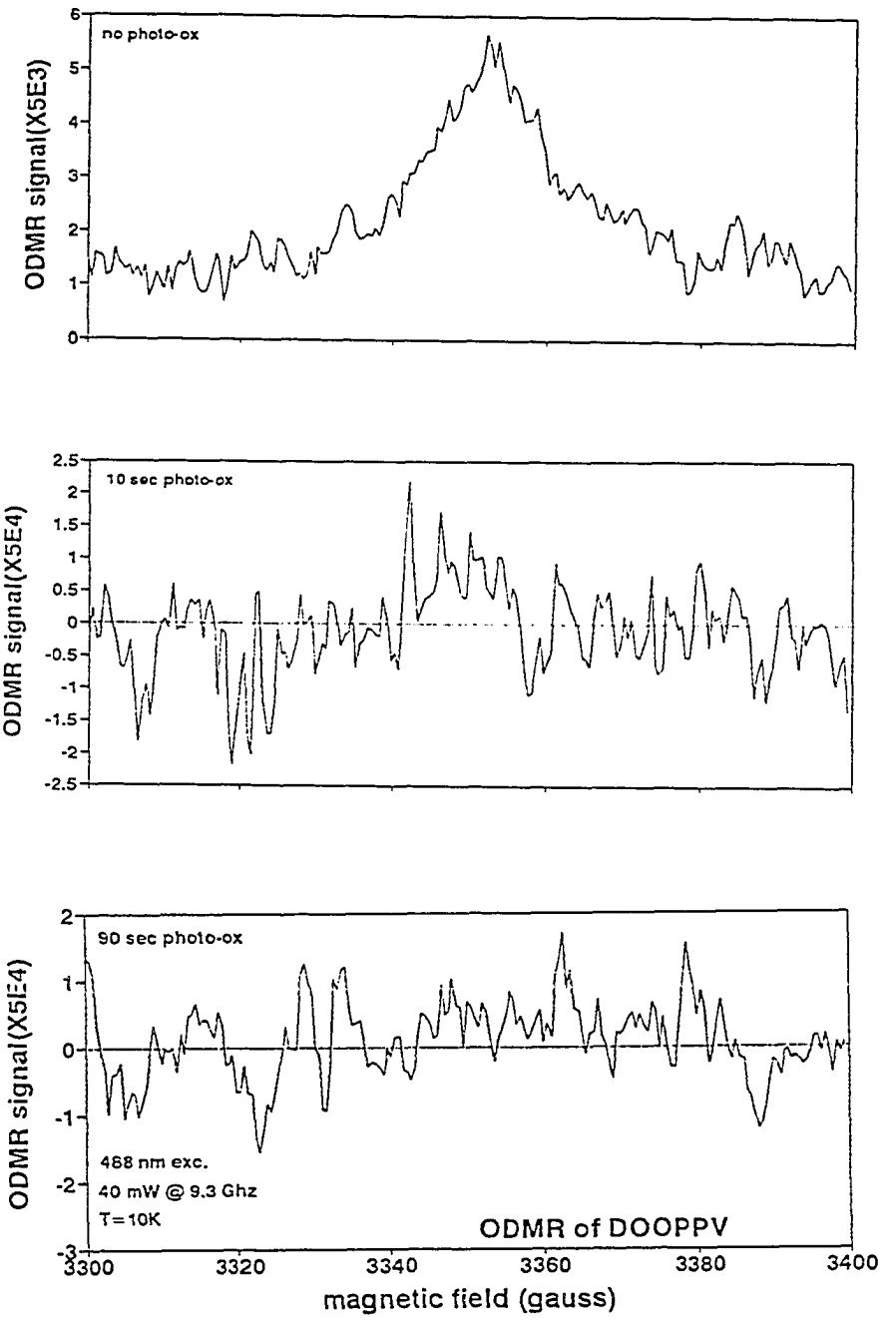

Figure 29
Effects of photo-oxidation on the narrow resonance of DOOPPV excited at λ_{ex} =488 nm

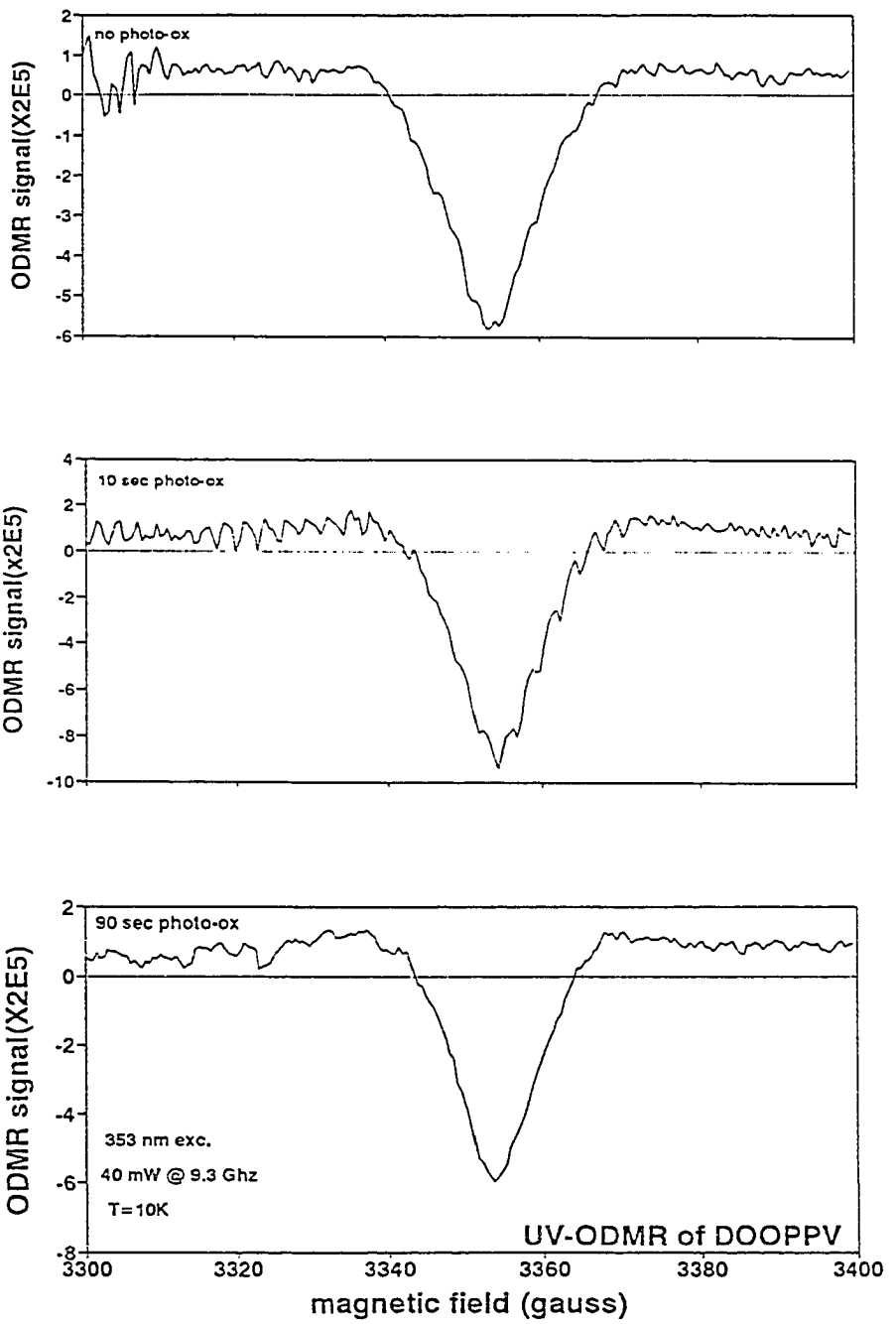

Figure 30
Effects of photo-oxidation on the narrow resonance of DOOPPV excited at λ_{ex} ~353 nm

resonance at λ_{ex} ~353 nm remaining unchanged under exposure to incident radiation in the presence of an oxygen atmosphere. Likewise, Figure 31 shows that at λ_{ex} ~308 nm, the scenario is the same with no resolvable decrease in the intensity of the PL-quenching peak due to the effects of photo-oxidation.

These results are fairly conclusive. The narrow PL-enhancing PLDMR in DOOPPV films is quenched dramatically upon photo-oxidation. The PL-quenching resonance observed using UV-excitation appears to be unaffected by photo-oxidation of those films.

PLDMR Study of Unsubstituted PPV and CN-PPV Films

The narrow PLDMR spectra were measured in the unsubstituted PPV using λ_{ex} = 488 nm and λ_{ex} ~353 nm (Figure 32). Two obviously unique results are striking: (i) The linewidth, $\Delta H_{1/2}$, is much broader ($\Delta H_{1/2} \approx$ 30 gauss) than normal ($\Delta H_{1/2}$ ~ 15 gauss) in both of the spectra. (ii) The narrow polaron resonance exhibits a PL-enhancing characteristic at λ_{ex} ~353 nm. All other PPV films studied to date using UV excitation show a clear PL-quenching, narrow resonance. Next, the broad full-field and half-field triplet powder pattern resonances are undetectable at λ_{ex} = 488 nm or λ_{ex} ~353 nm. The spectra appear in Figure 33.

The cyano substituted PPV film has similar PLDMR features to the other substituted PPV films studied. The narrow polaron resonance excited at λ_{ex} = 488 nm shows a strong PL-enhancing characteristic. The same spectrum, when excited with λ_{ex} ~353 nm, exhibits a

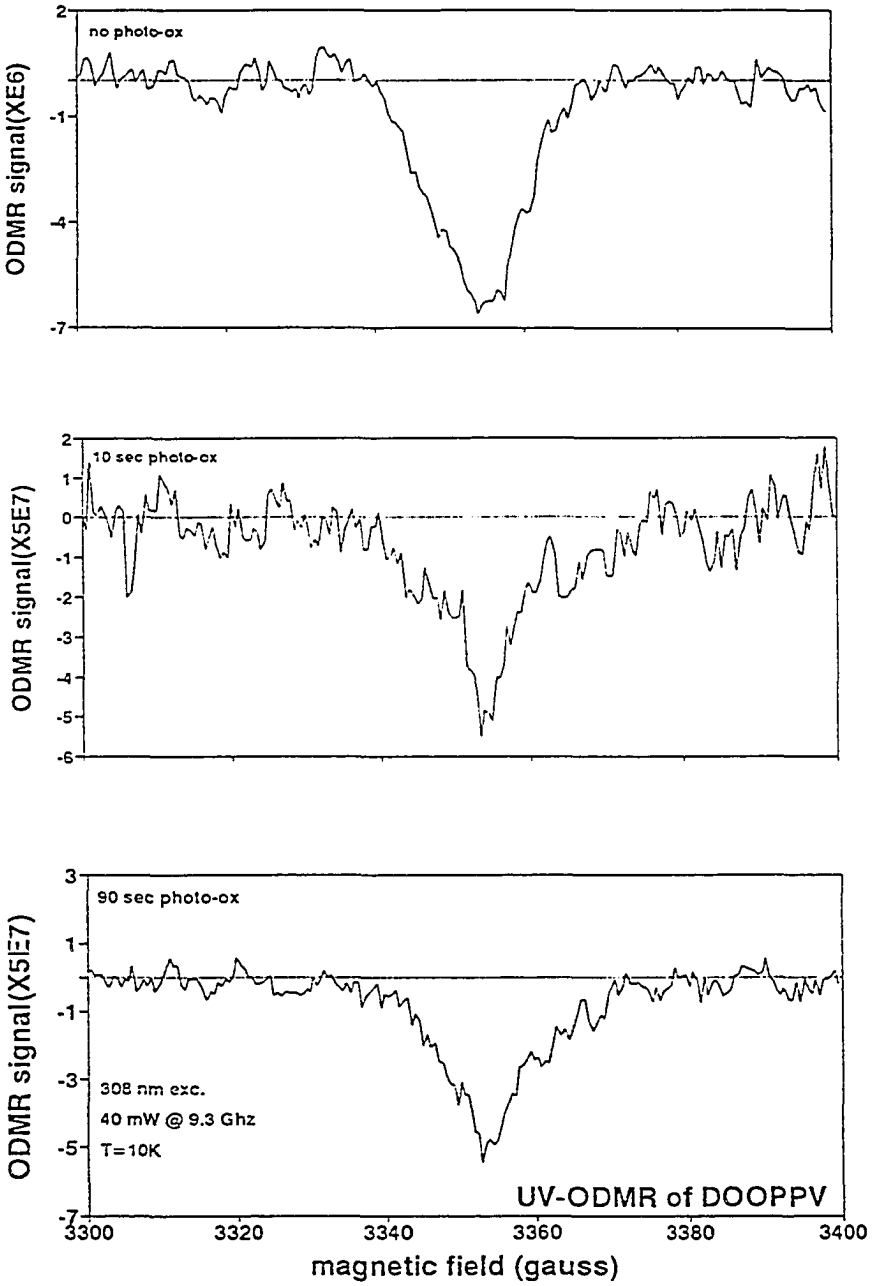

Figure 31
Effects of photo-oxidation on the narrow resonance in DOOPPV excited at λ_{ex} ~308 nm

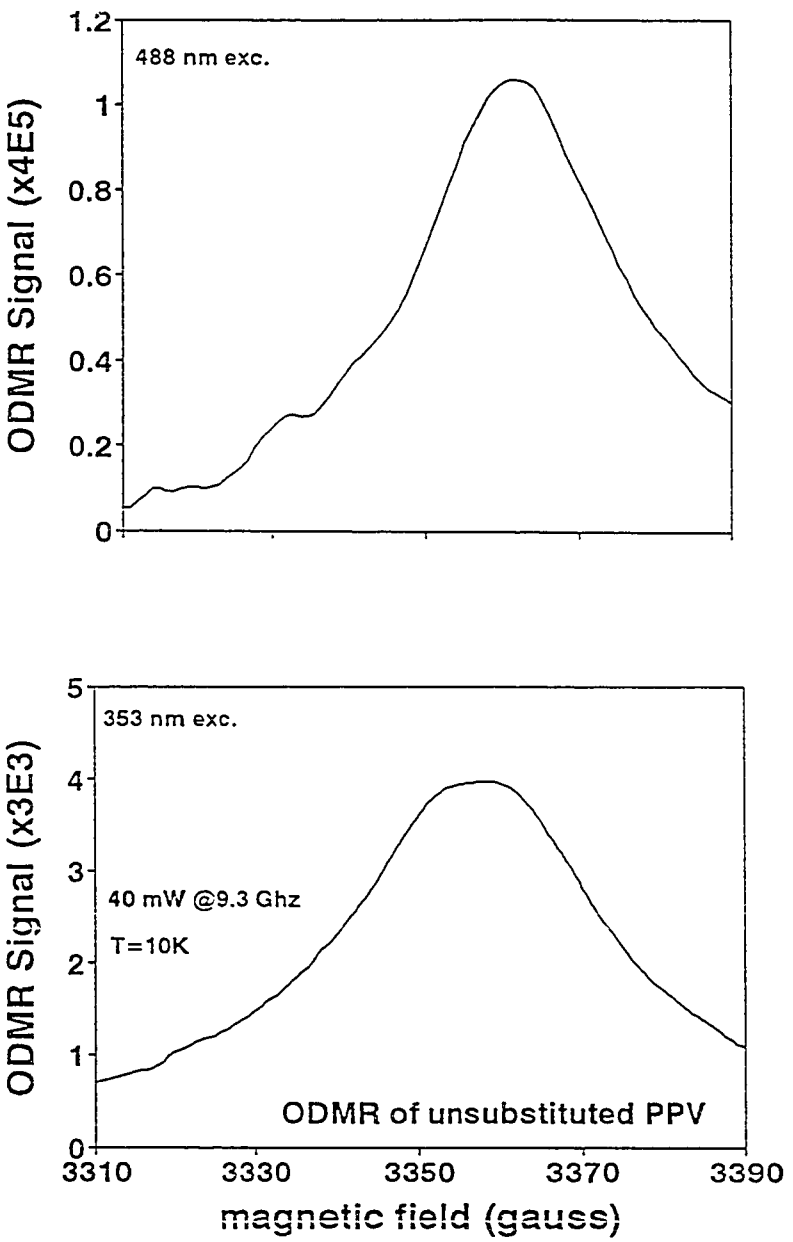

Figure 32
Narrow polaron resonance of unsubstituted
PPV film excited at $\lambda_{ex} = 488$ nm and λ_{ex} ~353 nm

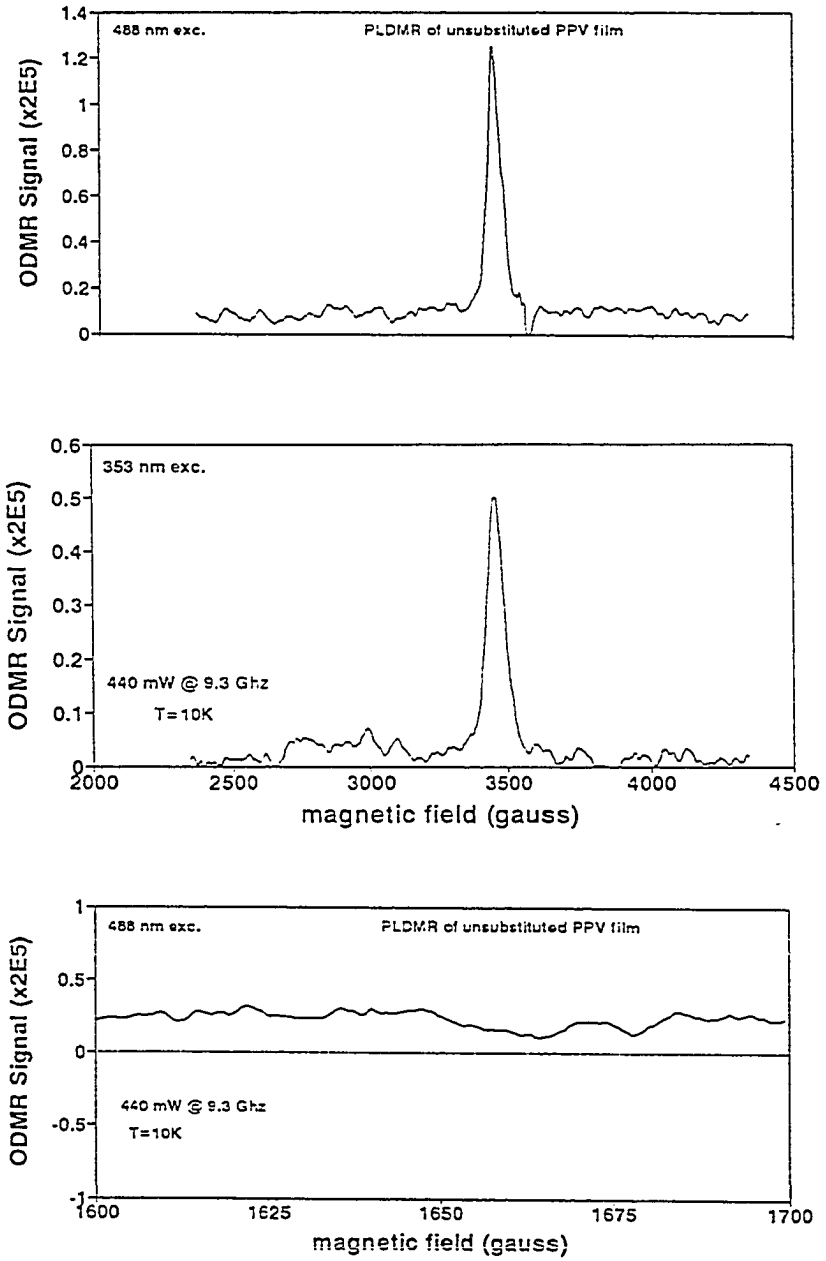

Figure 33
Full- and half-field triplet powder pattern PLDMR of the unsubstituted PPV film excited at λ_{ex} = 488 nm and the full-field spectrum excited at λ_{ex} ~353 nm

strong PL-quenching feature not unlike DHOPPV and DOOPPV as well as the P3ATs (see earlier in this thesis). These spectra are shown in Figure 34. The full-field triplet powder pattern measured at λ_{ex} = 488 nm was very strong. The diminishing of the intensity of the triplet resonance at higher excitation source energies is not unique to this sample. The spectra at λ_{ex} = 488 nm and those UV-excited at λ_{ex} ~353 and 308 nm are shown in Figure 35. An interesting feature related to the narrow polaron resonance upon laser excitation at λ_{ex} = 488 nm is observed. It seems that the onset of a PL-quenching narrow resonance appears at centerfield. A possible scenario for recording the feature in this spectrum and not in Figure 34 is that some photochemistry may be taking place *in-situ*. This hypothesis is speculative at best. Note the strong PL-enhancing characteristic of the narrow resonance in the spectrum taken at λ_{ex} ~353 nm. The half-field spectrum using λ_{ex} = 488 nm is shown in Figure 36 as well as the temperature dependence of the half-field in the temperature range $15 \leq T \leq 135$ K. The intensity is still very strong at T = 135 K.

PLDMR Studies of Poly(di(phenyleneethynylene)phenylene-vinylene) (PDPEPV) and CN-PDPEPV Films

The narrow PLDMR spectra were measured in the Poly(di(phenyleneethynylene)-phenylenevinylene) (PDPEPV) film (see Figure 6) at λ_{ex} = 488, ~353, ~308, and ~250 nm (Figure 37). There are three features which stand out: (i) At λ_{ex} = 488 nm, $\Delta H_{1/2}$ is much narrower ($\Delta H_{1/2} \approx 3$ G) than any narrow resonance linewidth measured to date. (ii) As in the

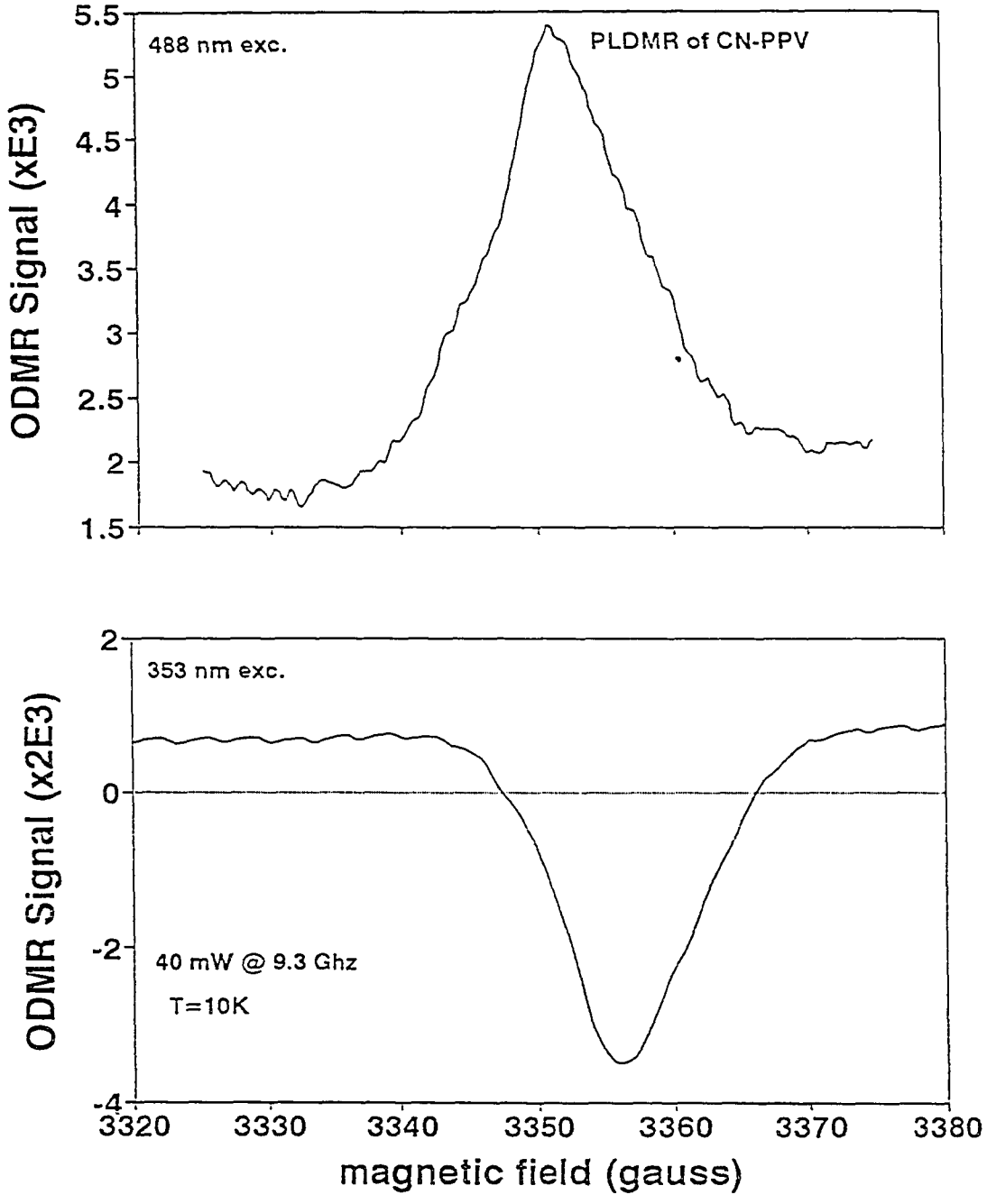

Figure 34
Narrow, polaron resonance in cyano substituted
the PPV film excited at $\lambda_{ex} = 488$ nm and λ_{ex} ~353 nm

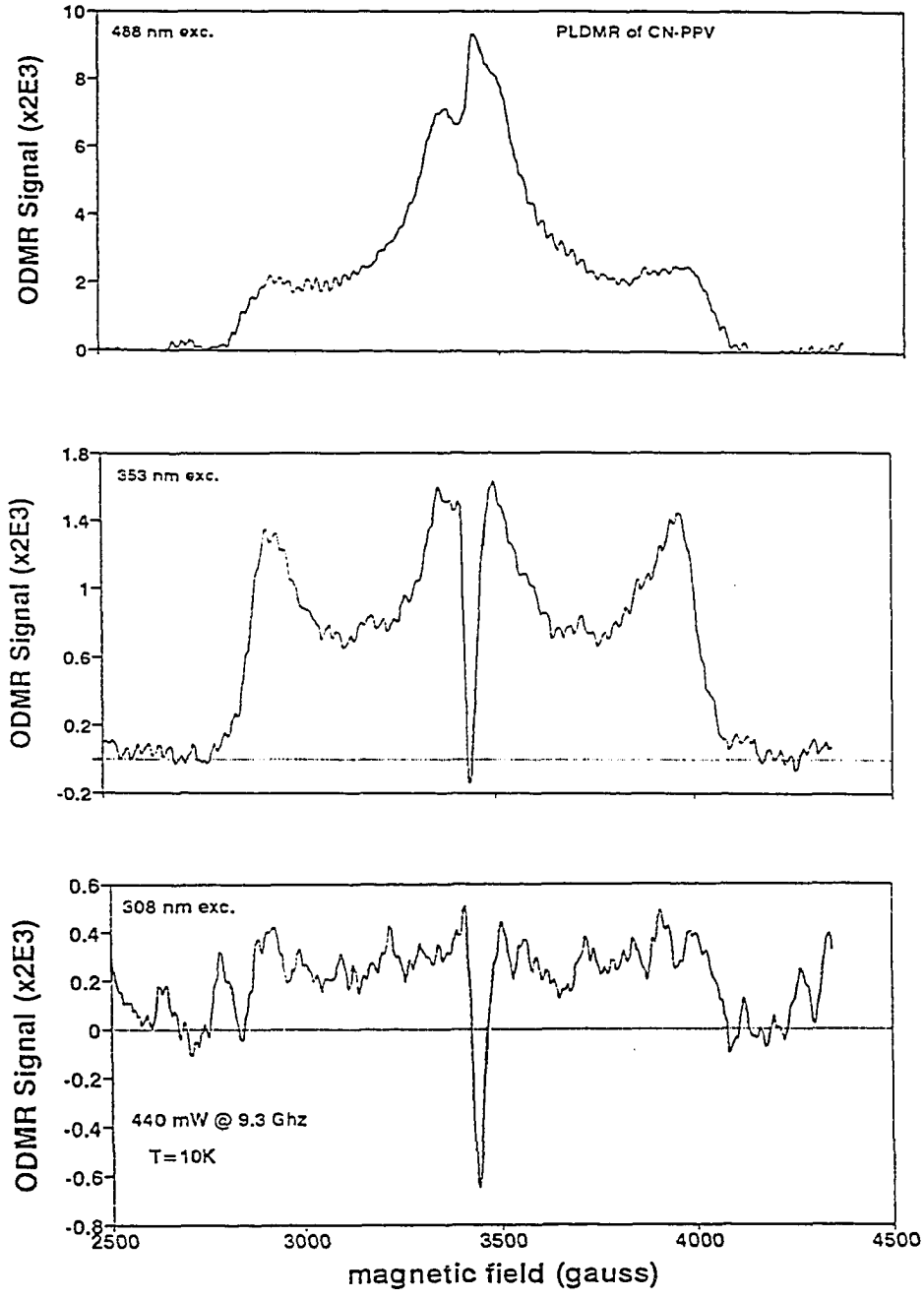

Figure 35
Full-field triplet powder pattern of the cyano substituted PPV film excited at λ_{ex} = 488 nm and λ_{ex} ~353 and 308 nm

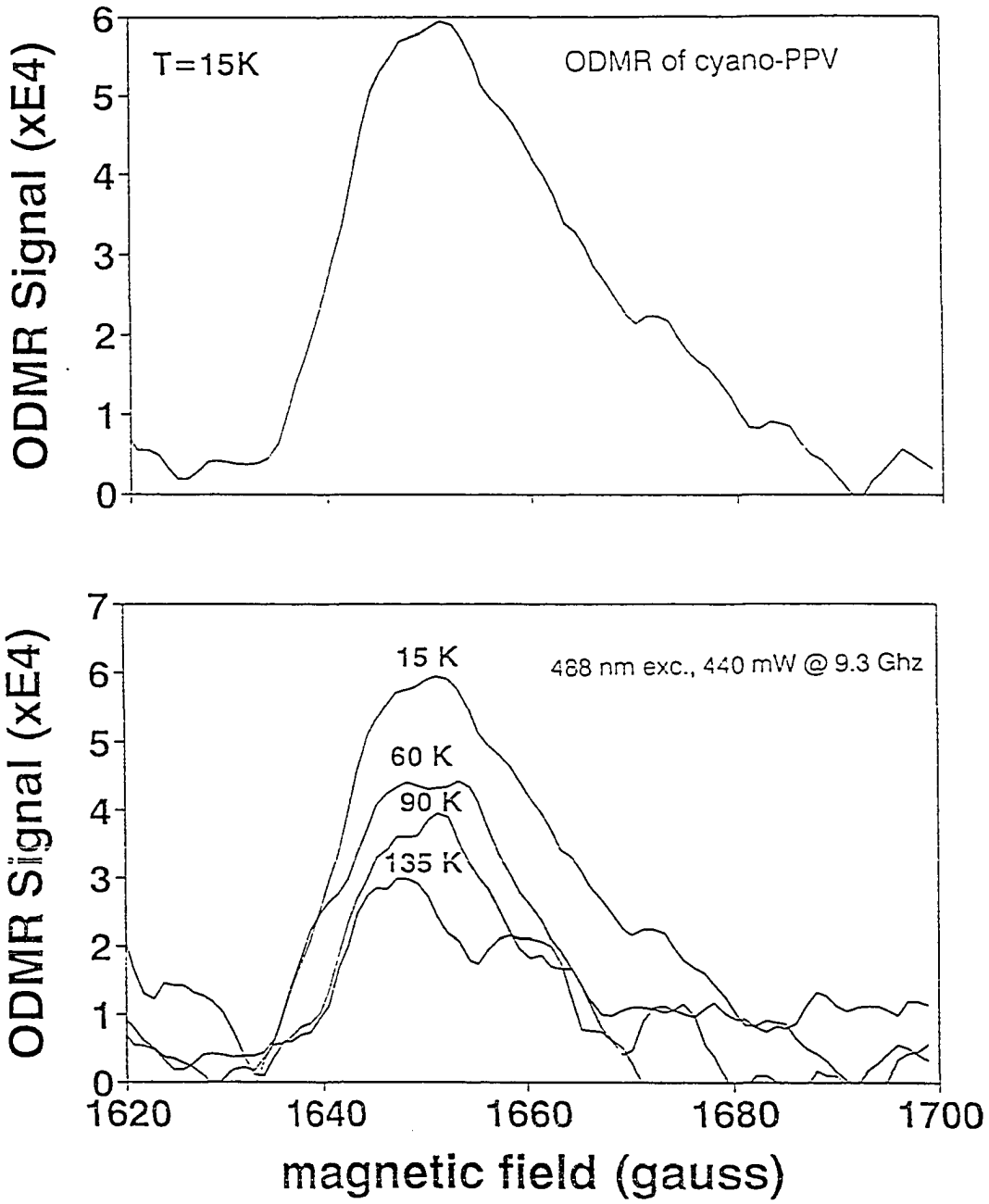

Figure 36
Half-field spectrum and temperature dependence of cyano substituted PPV film excited at $\lambda_{ex} = 488$ nm

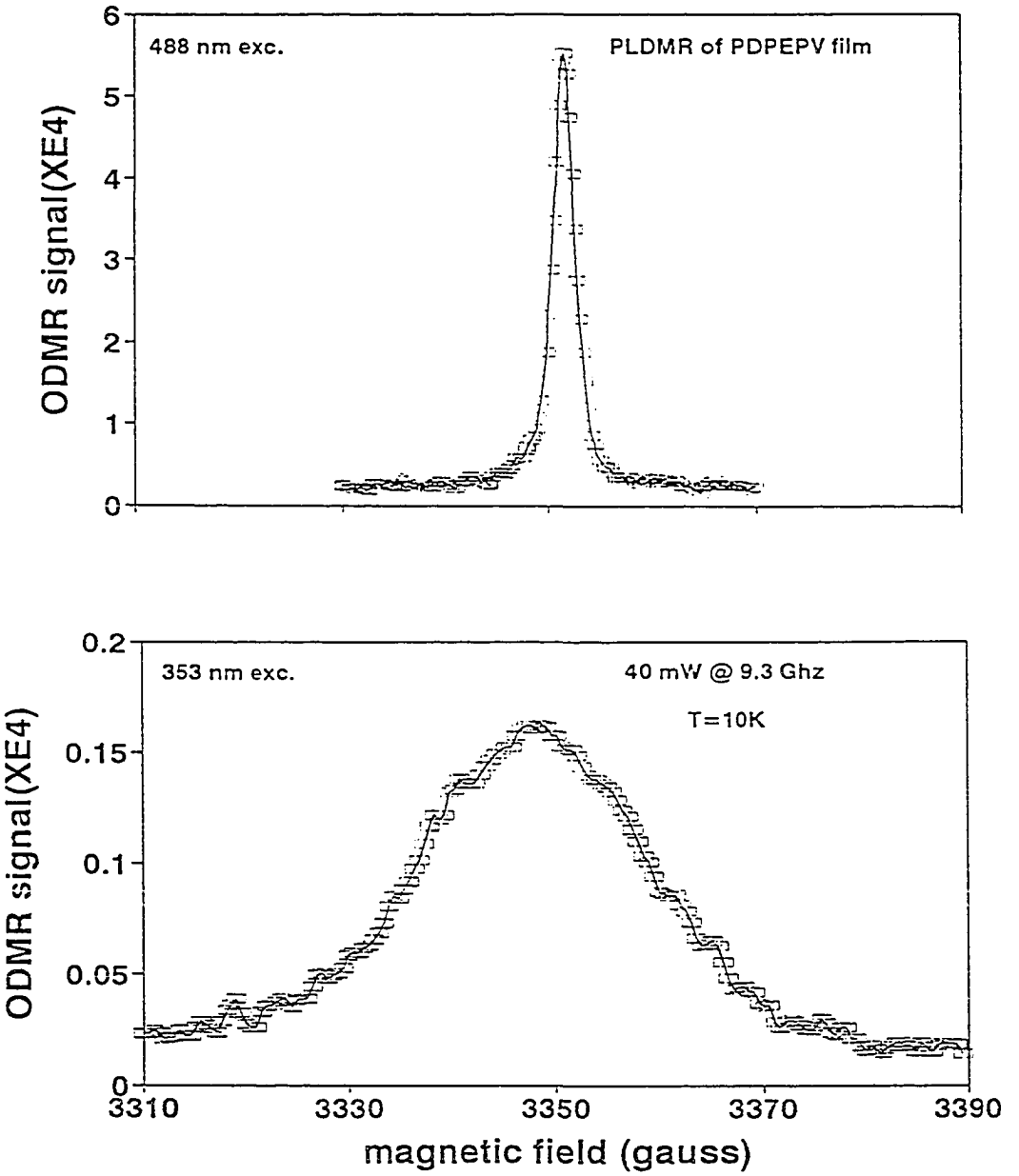

Figure 37
Narrow polaron resonance of PDPEPV at
λ_{ex} = (a) 488, ~353, (b) 308 and 250 nm

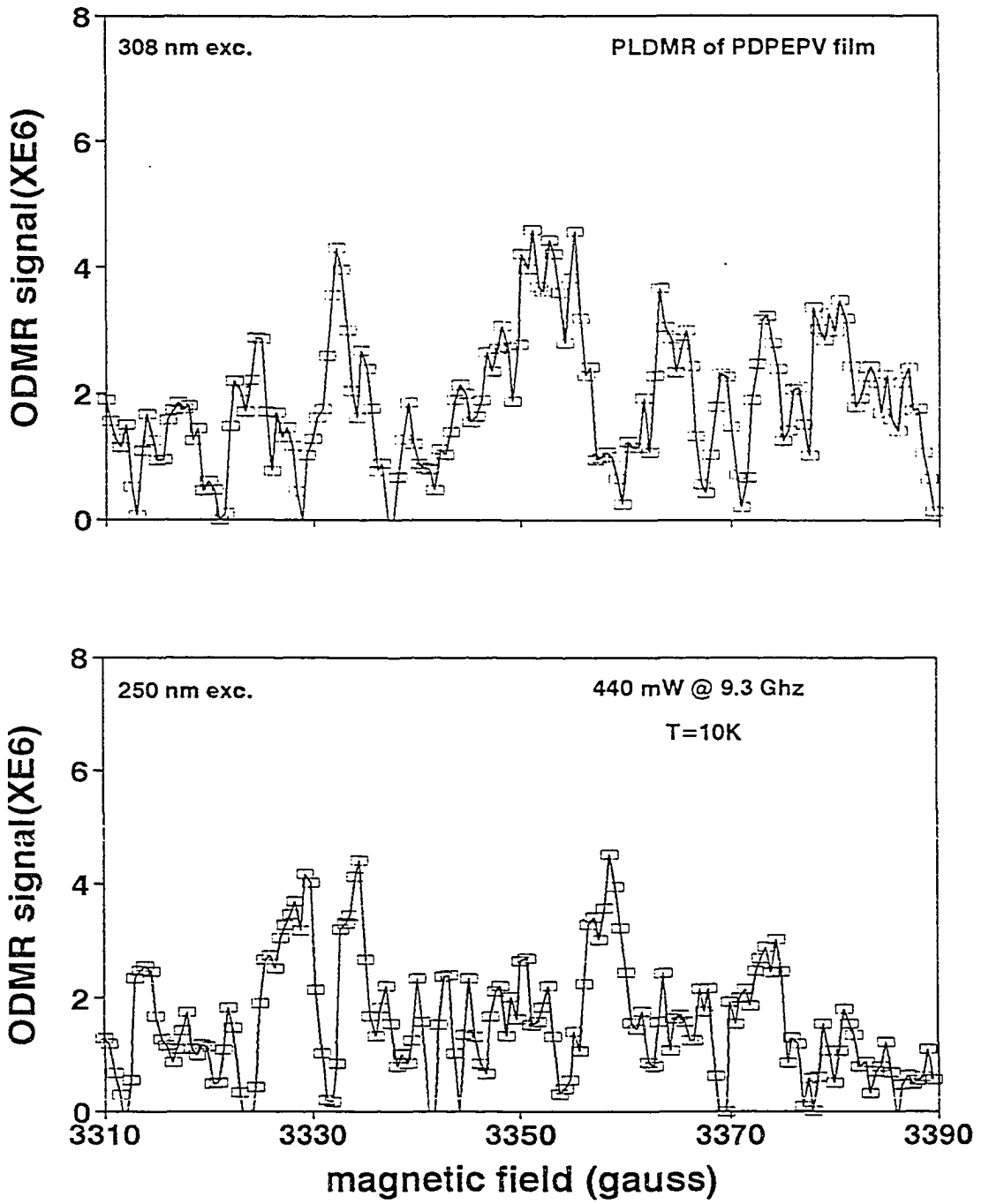

Figure 37 (continued)

unsubstituted PPV, the narrow polaron resonance exhibits a PL-enhancing characteristic at λ_{ex} ~353 nm. The linewidth is much broader ($\Delta H_{1/2} \approx 24$ G) than that measured at $\lambda_{ex} = 488$ nm. (iii) The spectra at λ_{ex} ~308 and 250 nm show neither a PL-enhancing feature as in PPA and PPEA nor a PL-quenching feature as in substituted PPV and P3AT films. Unlike the unsubstituted PPV film, however, PDPEPV exhibits a clear triplet powder pattern at full- and half-field (see Figure 38).

The CN-PDPEPV film exhibits characteristics in its narrow polaron resonance (Figure 39) measured at $\lambda_{ex} = 488$ and ~353 nm similar to those of the substituted PPV films including CN-PPV and P3ATs. A PL-enhancing narrow resonance is observed at $\lambda_{ex} = 488$ nm whereas a PL-quenching feature is observed at λ_{ex} ~353 nm.

ESR and Light-induced ESR (LESR) of Poly(p-phenylenecumulenes) (PPC)

The ESR of the undoped and iodine-doped PPC (Figure 5, top) is shown in Figure 40. The ESR spin density of the undoped polymer is very low, $N_s = 3.4 \times 10^{14}$ spins/gram (2.7×10^{-7} spins per repeat unit), and the derivative peak-to-peak width is $\Delta H_{pp} \approx 2.7$ gauss. They are essentially nonluminescent. Upon exposure of the PPC to iodine vapor at room temperature, N_s increases to ~1.2×10^{17} spins/gram (1 per 10^4 repeat units), and ΔH_{pp} increases to 5.9 gauss. Finally, the PPC also exhibited a light-induced ESR (see Figure 41).

Two similar, yet uniquely different, polymers were obtained from the chemistry group

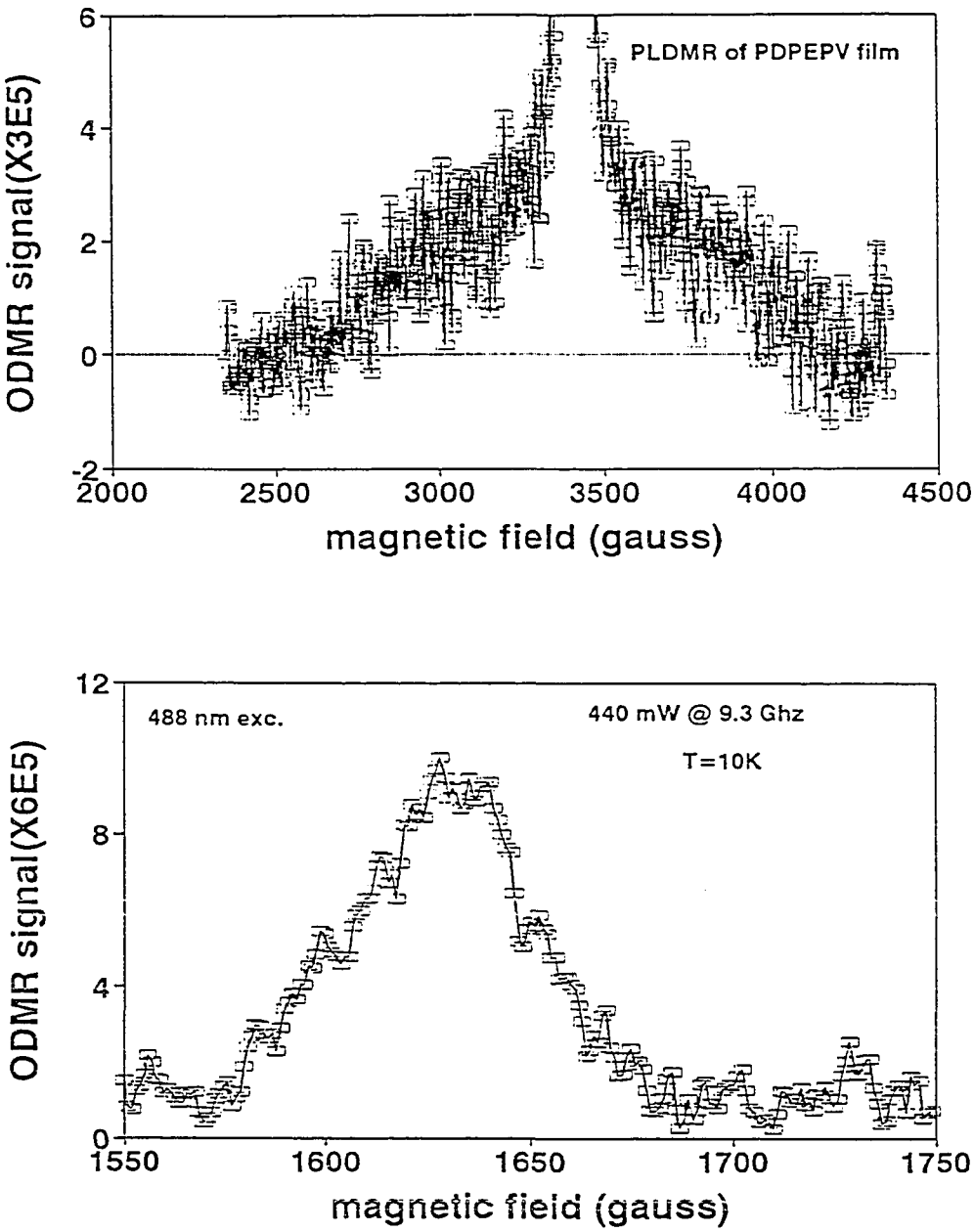

Figure 38
Full- and half-field triplet powder pattern
PLDMR of PDPEPV film at λ_{ex} = 488 nm

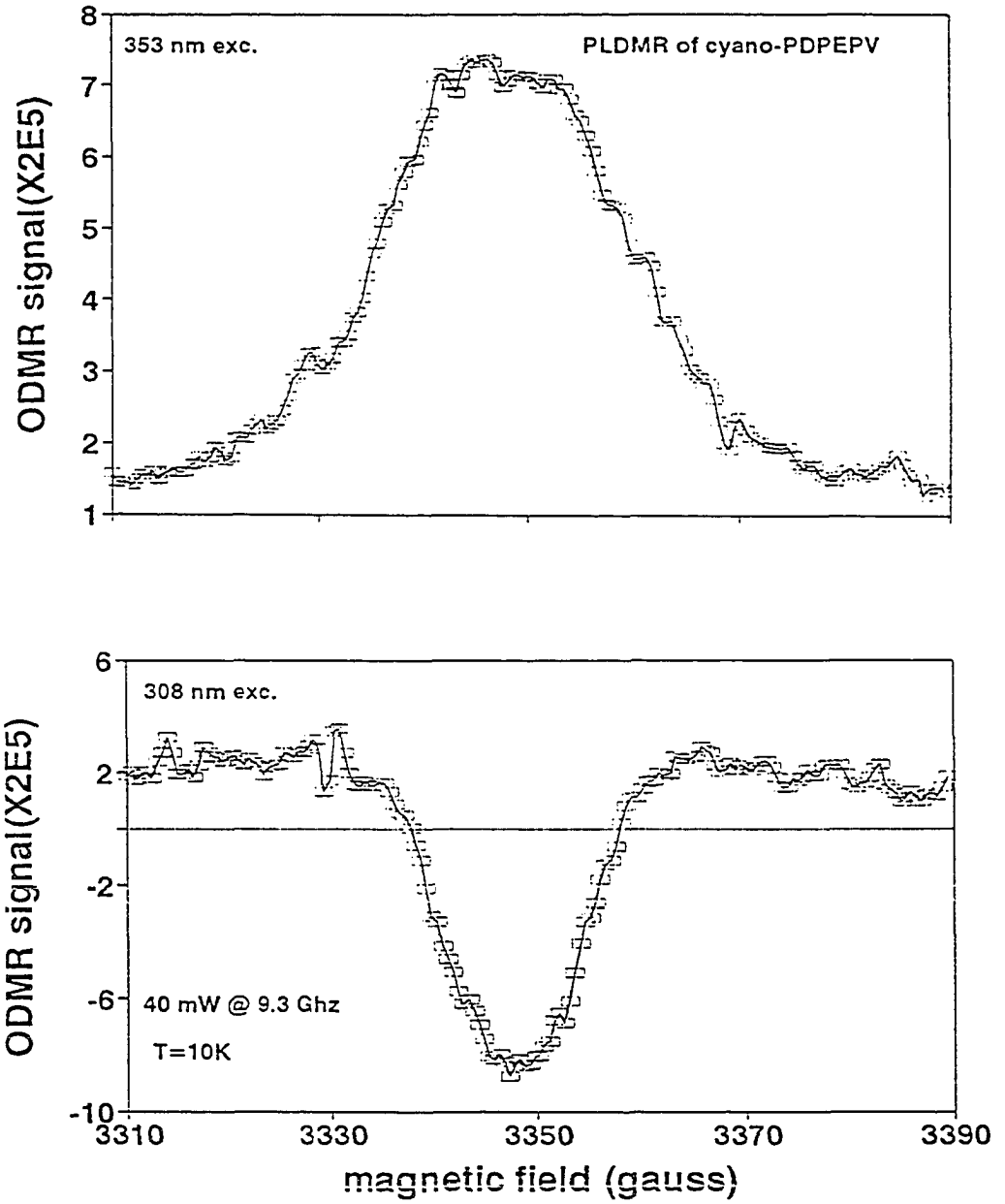

Figure 39
Narrow polaron resonance of CN-PDPEPV
film at λ_{ex} = 488 and ~353 nm

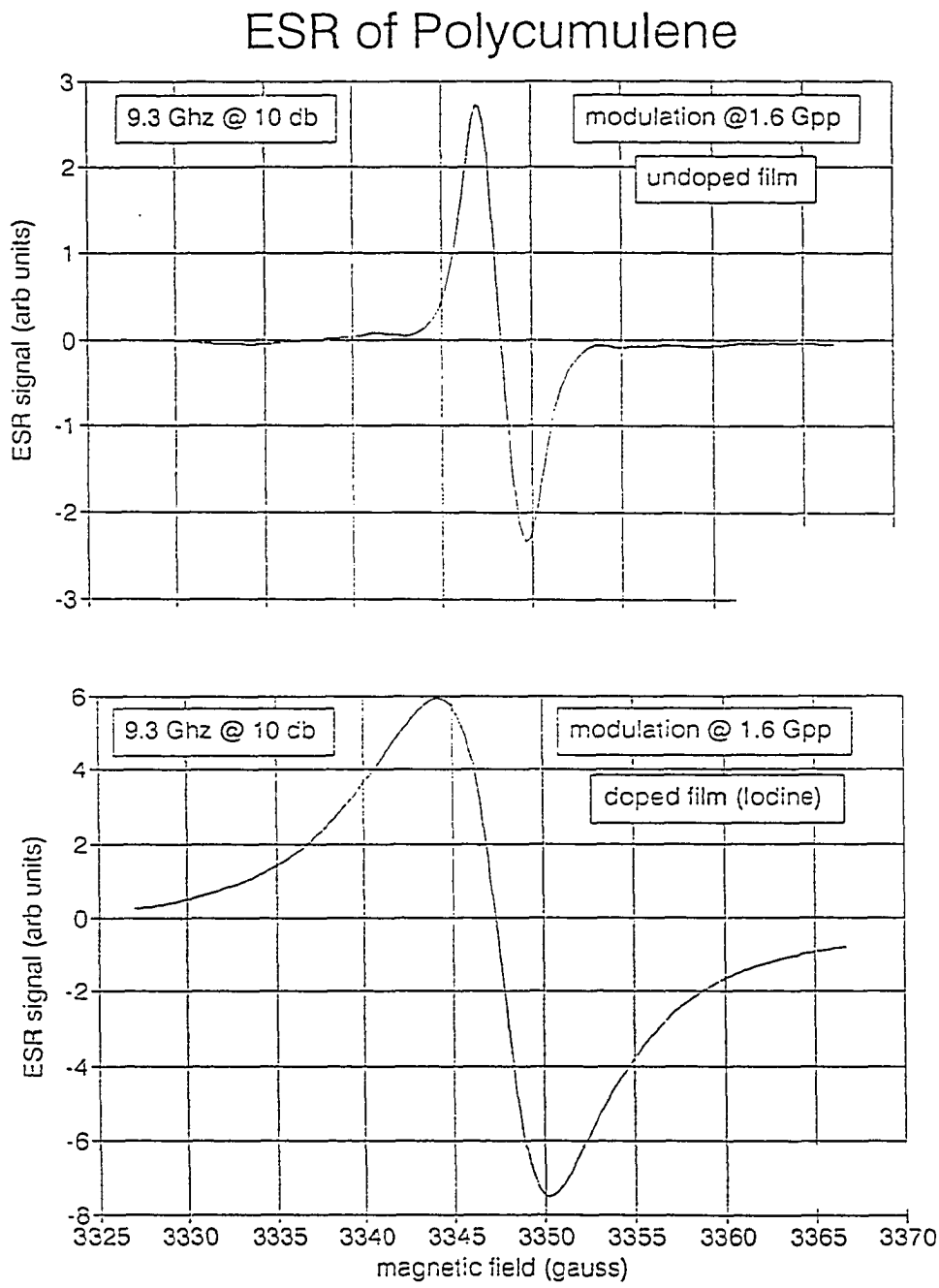

Figure 40
ESR of undoped and
iodine-doped PPC

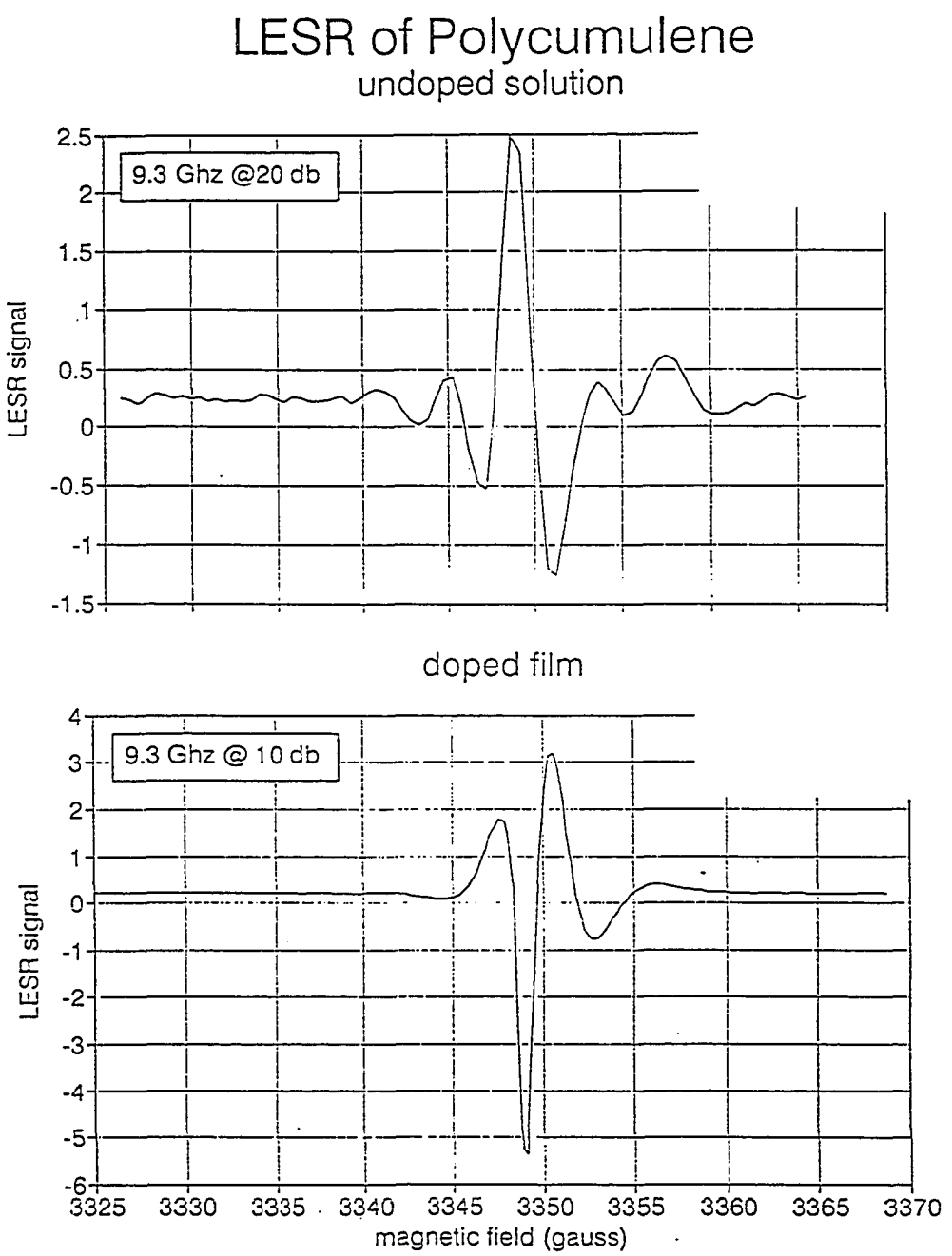

Figure 41
LESR of undoped and
iodine-doped PPC

of T. J. Barton at Iowa State University and the Ames laboratory. The representations of these polymers are shown as the bottom two structures of Figure 5. The photoluminescence spectra were taken and shown in Figure 42. The simple observation that the 1,3 butadiene polymer luminesces brightly while the 1,2,3 butatriene does not is significant.

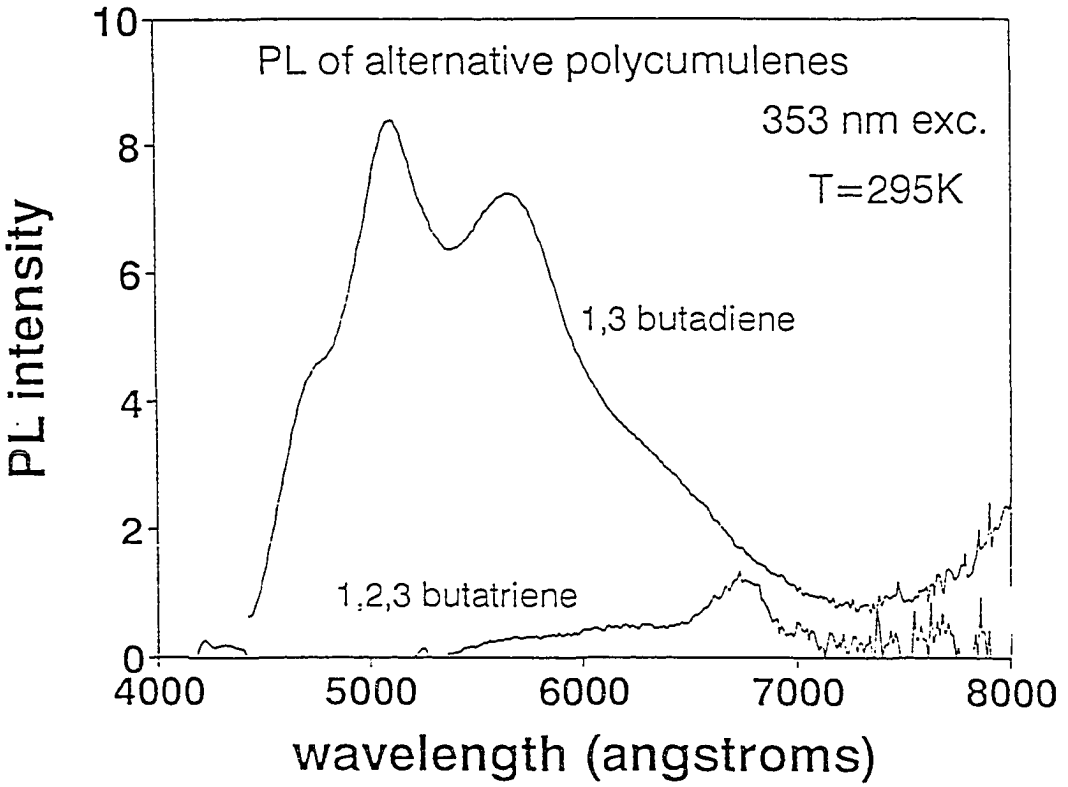

Figure 42
Photoluminescence spectra of the alternative polycumulenes

DISCUSSION

Poly(p-phenyleneethynyleneaniline) (PPEA)

The salient observations from the experiments performed on the PPEA derivatives described above offer several interesting, but at present tentative, suggestions on the nature of these polymers:

(i) The phonon sidebands of the PL of solutions is consistent with the C≡C stretch vibration energy. However, since very few progressions are observable, the assignment of this structure to that vibration mode is clearly speculative. Still, the general observation of greater structure in solutions rather than films is striking. It may be argued that the triple bond-based backbones are much more rigid than double bond-based chains and the solvent consequently induces fewer dynamical structural defects which disrupt the conjugation. Casting onto films may then induce far more static structural defects than in the more flexible double-bonded backbones, which may relax during the casting process.

(ii) Similar to PPAs[39] but in contrast to PPVs[38] and P3ATs[37], the narrow PL-enhancing polaron PLDMR is very wide and short λ_{ex} does not induce a PL-quenching resonance (see above). This behavior is also consistent with a large density of structural defects in the films, if these structural defects stabilize polarons and thus enhance their steady-state population. Although higher energy neutral and charged excitations are photogenerated at short λ_{ex}, the high density of these structural defects may relax a large number of these

excitations into polaron states similar to those generated at visible λ_{ex}, resulting in a λ_{ex}-independent polaron PLDMR.

(iii) The ~ 1500 G width of the full-field triplet exciton powder pattern PLDMR is also consistent with a large density of structural defects, if it is assumed that the triplet excitons may become stabilized by these structural defects. If this scenario is vindicated, it would explain the broad distribution of triplet ZFS parameters in general and of the parameter **E** which is a measure of the deviation from axial symmetry in particular, which result in the broad, relatively structureless pattern.

(iv) Finally, the drastic reduction in the intensity of the triplet exciton pattern at short λ_{ex} is similar to the behavior of PPVs and P3ATs (see above). It is suspected that the major triplet exciton generation mechanism is intersystem crossing from the (rigid) singlet 1^1B_u exciton which is the dominant photogenerated excitation at longer λ_{ex}. Thus, short λ_{ex} generates higher energy excitations and the quantum yield of the 1^1B_u exciton, which is the source of both the PL and the 1^3B_u triplet excitons, sharply decreases. The observed reduction of the PL at short λ_{ex}, which is indeed observed in other systems as well as in the PPEAs, is clearly consistent with this scenario.

The Interband versus Exciton Models

The narrow PL-enhancing resonance in conjugated polymers previously obtained and studied by visible excitation was attributed to magnetic resonance enhancement of singlet

exciton generation by p^+ - p^- fusion.[7-9,37-41] However, it is difficult to explain the narrow PL-quenching resonance observed by UV excitation within this picture. We therefore reexamine the nature of the narrow PL-enhancing resonance. In searching for an alternative model, we consider the substantial evidence for the role of polarons and bipolarons as singlet exciton quenching centers.[40,42-43] The PL-enhancing resonance may indeed result from the spin-dependent p^+ - p^- recombination, but that recombination probably results in a nonradiative decay. It, would, however, enhance the PL of the polymer by removal of these nonradiative quenching centers from the system. The PL-quenching resonance observed by UV excitation might be explained by considering the nature of the photogenerated excitations. These probably include high-energy neutral species as well as charged electron- and hole-like species which can decay into the 1^1B_u singlet exciton, providing the source of the nongeminate luminescence. The spin- dependent capture of the charged excitations by p^+ and p^- trapping centers would then reduce the rate of their relaxation into the 1^1B_u state and reduce the PL. This mechanism might also account for, or contribute to, the electroluminescence (EL)-quenching resonance exhibited by PPV- and PPA-based LEDs, which was previously attributed to the spin-dependent decay of like-charged polarons into bipolarons.[7-9,40] The absence of the PL-quenching resonance from PPA might then be due to structural defects in that system, which rapidly trap the various charged excitations into polaron states. The dominant role of polarons as nonradiative singlet exciton quenching centers also provides a simple explanation for the strong quenching of the PL by doping, which generates stable polaron states on the chains.

Next, if the $1^1B_u \rightarrow 1^3B_u$ intersystem crossing is the major triplet exciton generation mechanism, the drastic reduction in the intensity of the triplet exciton resonance at short λ_{ex} in PPEA and as well as other conjugated polymers may be coupled to the strong reduction in the PL intensity. While visible photoexcitation directly produces geminate luminescent 1^1B_u excitons, UV excitation generates higher-energy states, which relax to the 1^1B_u state at a much lower rate.

Finally, the scenario in which defect-stabilized polarons and bipolarons are the dominant nonradiative quenching centers of charge carriers in LEDs may provide striking insight into their performance and stability. If this picture is validated, then the possibility that the nonradiative recombination of the carriers with polarons and bipolarons generates defects in a mechanism similar to the Staebler-Wronski effect in hydrogenated amorphous Si should be considered.

The fact that the onset of the PL-quenching resonance occurs in the range $2.71 \leq E_{ex} \leq 2.88$ eV in DHOPPV films and in the range $2.88 \leq E_{ex} \leq 3.05$ eV in DOOPPV and P3AT films is very important. The absorption band edge in these films is clearly below 2.4 eV. If we consider that the band edge is where the photo-absorption into the ^1B_u singlet exciton state begins and the onset of the PL-quenching resonance is at the continuum band edge, then we can calculate a lower bound on the binding energy of the singlet exciton. For DHOPPV this value is ~ 0.3 eV and for the DOOPPV and the P3ATs it is ~0.5 eV. These values for the binding energy of the singlet exciton are similar to those reported elsewhere.[23,44] The fact that this binding energy is so large relative to k_BT at temperatures of interest is

significant. It strongly suggests that the fundamental absorption edge is a ground state to singlet exciton state excitation and **not** a band-to-band transition.

The Nature of the Narrow PL-enhancing Polaron Resonance

We know that the PL which remains after the quenching of singlet excitons at defect sites created by the effects of the photo-oxidation is due to rapidly decaying singlet excitons.[35] These excitons are not as susceptible to quenching at these defect sites as the more slowly decaying species are. They are further not as susceptible to quenching at polaron defect sites. The role of polarons as quenching centers for singlets is then reduced. Thus, their enhanced removal from the system at resonance should not affect the PL as much as it did before photo-oxidation. The net result in the data showing that the narrow enhancing PLDMR decreases with photo-oxidation supports the picture that polarons are responsible for the PL-enhancing feature, but not as was previously thought.

The model that resonance conditions enhance the fusion of p^+ - p^- pairs which decay radiatively yielding increased photo-luminescence does not seem to be supported by the photo-oxidation results described above. Rather, the competing picture is that polarons act as nonradiative quenching centers for singlets. Under resonance conditions their removal from the system by nonradiative recombination is enhanced thereby allowing more singlets to decay radiaitively. The PL-enhancing narrow resonance could be explained via this mechanism and is supported by the photo-oxidation results described above.

The Nature of the Electroluminescence in PPV/CN-PPV LEDs

The half-field resonance in the ELDMR of PPV/CN-PPV LEDs appears at very high temperatures. In contrast, the triplet resonance in the unsubstituted PPV is known to attenuate quickly with increasing temperature. The experiments which show that the half-field resonance of CN-PPV appears at temperatures as high as 135 °K indicate that the CN-PPV layer of the PPV/CN-PPV diodes is respnsible for the measured EL.

Poly(p-phenylenecumulenes) (PPC)

It is interesting to compare the behaviour of the ESR of the PPC to that of polydiethynylsilanes (PDES)[36], since these latter polymers exhibit similar behaviour to that of PPC: Their undoped and doped conductivities are similar, and they are also essentially nonluminescent. In the undoped PDES prepared from hydrogenated precursors, $\Delta H_{pp} \approx 10$ gauss, and the spin density is ~1 spin per ~14,000 repeat units. However, when the PDES is prepared from deuterated precursors $\Delta H_{pp} \approx 3.6$ gauss. It therefore appears that in the PDES, the major source of the linewidth is the hyperfine coupling with protons. The narrow ESR linewidths of the undoped PPC therefore suggests that the hyperfine coupling with protons is very weak. This observation and conclusion are consistent with the localization of the spin defects on the -C=C=C=C- segments of the PPC. In PDES prepared from hydrogenated precursors, addition of iodine to PDES solutions initially decreases ΔH_{pp} to

~3.4 gauss. However, upon heavier doping of up to 40 wt.%, ΔH_{pp} increases to ~7 gauss. It therefore appears that the behaviour of the doping induced ESR of PPC is similar.

The temperature dependence of the doping-induced ESR of PDES indicated that it was motionally narrowed above ~100 °K, with an activation energy $E_a \approx 3.7$ meV. The strikingly similar behaviour of the PPC and PDES suggests a similar electronic structure. The absence of photoluminescence in these polymers, similar to t-$(CH)_x$, but in contrast to many other π-conjugated systems, such as polythiophenes and poly(*p*-phenylenevinylenes), etc., is consistent with the hypothesis that the lowest singlet excited state is the single photon dipole forbidden 2^1A_g. In the luminescent polymers, it is widely believed that the lowest excited singlet state is the single photon dipole allowed ^1B_u. Various nonlinear optical measurements by Vardeny and coworkers are currently underway to examine this hypothesis and determine the electronic structure in detail and will be published later.[45]

The photoluminescence spectra of the 1,3 butadiene and 1,2,3 butatriene polymers (figure 5, bottom) were shown in figure 42. Obviously, the difference in the structure of the two polymers resides in the breaking of the central double bond in the luminescent one with subsequent attachment of hydrogens to satisfy the dangling bonds. The C=C=C=C sequence in the non-luminescent polymer obviously has zero alternation ($\delta = 0$) in that portion of its backbone. The same area in the modified, luminescent system exhibits a high degree of electronic alternation.

This result lends credence to the theory evolving about the role of δ in the ordering of the excitonic levels within π conjugated systems.[22] However, the conclusion remains

somewhat tenuous. There are systems such as polydiacetylene (PDA) in which high alternation exists and yet no luminescence is detected from these. This suggests that there are other considerations involved in determining the relative ordering of the excitonic levels in these systems including electron-electron correlation.[22]

SUMMARY AND CONCLUSIONS

The novel approach of using ultraviolet excitation in performing photoluminescence detected magnetic resonance (PLDMR) experiments has opened new doors to investigations of the optical and magnetic resonance properties of π-conjugated polymers. First, polymers whose bandgaps are too high for photo-excitation at visible wavelengths are now being studied. Next, the PLDMR signatures of many other polymers with lower gaps is λ_{ex} - dependent and differences in their PLDMR spectra have led to a better understanding of their physical properties.

The photoluminescence (PL), electron spin resonance (ESR) and X-band UVODMR of poly(*p*-phenyleneethynyleneaniline) (PPEA) derivatives are discussed. PPEA is a high gap polymer not studied before using laser excitation. A strong PL-enhancing narrow resonance is observed at λ_{ex} ~353, 308 and 250 nm. Strong triplet full- and half-field powder pattern spectra are also observed at λ_{ex} ~353 nm. These spectra are severely diminished in intensity, however, upon excitation at higher incident energies. The ESR of undoped and iodine-doped films are also reported.

The UVODMR results on the poly(*p*-phenylenevinylene) (PPV), poly(*p*-phenyleneacetylene) (PPA), and poly(3-alkylthiophenes) (P3ATs) are most interesting. The PPV and P3AT derivatives show a departure from the results obtained using λ_{ex} = 488 nm.[27-29] All of these polymers show a PL-quenching resonance which onsets in the region 406nm $\leq \lambda_{ex} \leq$ 430 nm except for the dihexoxy (DHO)PPV which onsets at a somewhat

higher wavelength in the range 430 nm $\leq \lambda_{ex} \leq$ 458 nm. These values allow us to estimate a lower bound on the binding energies of their respective singlet excitons. In the PPVs, except for DHOPPV, and in the P3ATs, the value calculated for the lower bound on the singlet exciton is 0.3 eV. In DHOPPV, the value is 0.5 eV. These values are in agreement with work published elsewhere.[23,44] The conclusion is that the fundamental absorption edge is a ground state to singlet exciton state excitation in these π-conjugated polymers and not a band-to-band transition. In PPA, no quenching resonance is seen up to wavelengths as low as λ_{ex} ~250 nm. All of the triplet powder pattern spectra are diminished in intensity as higher incident energies of photo-excitation are used.

The effects of photo-oxidation on dioctoxy (DOO)PPV films were also studied. Photo-oxidation sharply quenches the PL-enhancing narrow resonance. The PL-quenching resonance observed at $\lambda_{ex} \leq$ 430 nm seems to remain unaffected, however. This data supports the theory that polarons act as nonradiative quenching centers for singlets. Under resonance conditions, their enhanced removal from the system by nonradiative recombination enhances the photoluminescence. Furthermore, the model that resonance conditions enhance the fusion of positive and negative polaron (p^+ - p^-) pairs which decay radiatively yielding enhanced PL is not supported by these results.

The PLDMR of unsubstituted PPV and cyano substituted PPV (CN-PPV) are shown. The absence of a PL-quenching resonance in the unsubstituted form is interesting. The CN-PPV spectra are quite similar to those of other substituted PPV films. The temperature dependence of the half-field resonances of these polymers suggests that the visible

electroluminescence (EL) observed in PPV/CN-PPV LEDs is due to emission from the cyano layer.

The PLDMR of poly(*p*-di(phenyleneethynylene)phenylenevinylene) (PDPEPV) and cyano substituted PDPEPV are shown. The existence of a PL-enhancing resonance at λ_{ex} ~353 nm and the absence of a PL-quenching resonance in the PDPEPV film is notable. The cyano substituted PDPEPV exhibits similar features to those of substituted PPV and P3AT films.

The ESR and LESR of undoped and iodine-doped poly(*p*-phenylenecumulene) (PPC) films were also explored. These results and the lack of luminescence properties in these materials makes them strikingly similar to PDES films.[36] Amazingly, by simply breaking the central of the double bonds in the C=C=C=C sequence, a bright photoluminescence was measured. This result was discussed in the context of the theoretical work pursued by Soos et. al.[20-22] His work and our experimental studies lend credence to the proposal that a high alternation (δ) in the electronic transfer integral is conducive to luminescence while a low δ is not due to the effect of δ on the relative ordering of the ^1B_u and ^2A_g excited states in conjugated polymers.

BIBLIOGRAPHY

1. J.H. Burroughes, D.D.C. Bradley, A.R. Brown, R.N. Marks, K. MacKay, R.H. Friend, P.L. Burns, and A.B. Holmes, *Nature*, **347**, 539 (1990).

2. G. Gustafsson et al., *Nature*, **357**, 477 (1992).

3. Z. Yang, I. Sokolick, and F.E. Karasz, *Macromol.*, **26**, 1188 (1993); I. Sokolick, Z. Yang, F. E. Karasz, and D. C. Morton, to be published.

4. A. R. Brown et al., *Appl. Phys. Lett.*, **61**, 2793 (1993).

5. Y. Ohmori, M. Uchida, K. Muro, and K. Yoshino, *Sol. St. Comm.*, **80**, 605 (1991); *Jpn. J. Appl. Phys.*, **30**, L1938 (1991); *ibid.*, L1941.

6. G. Grem, G. Leditsky, B. Ullrich, and G. Leising, *Adv. Mater.*, **4**, 36 (1992); *Syn. Met.*, **51**, 383 (1992).

7. L. S. Swanson, J. Shinar, A.R. Brown, D.D.C. Bradley, R.H. Friend, P.L. Burn, A. Kraft, and A.B. Holmes, *Syn. Met.*, **55-57**, 1 (1993).

8. L. S. Swanson et al., in *Electroluminescence: New Materials for Devices and Displays,* edited by E. M. Conwell et al., *SPIE Conf. Proc.*, **1910**, 101 (1993).

9. L. S. Swanson, J. Shinar, A.R. Brown, D.D.C. Bradley, R.H. Friend, P.L. Burn, A. Kraft, and A.B. Holmes, *Syn. Met.*, **55-57**, 241 (1993).

10. C. K. Chiang, C.R. Fincher, Jr., Y.W. Park, E.J. Louis, S.C. Gau, and A.G. MacDiarmid, *Phys. Rev. Lett.*, **39**, 1089 (1977).

11. R. E. Peierls, *Quantum Theory of Solids,* Clarendon, Oxford (1955).

12. W. P. Su, J. R. Schrieffer, and A. J. Heeger, *Phys. Rev. Lett.*, **42**, 1698 (1979).

13. W. P. Su, J. R. Schrieffer, and A. J. Heeger, *Phys. Rev. B*, **22**, 2099 (1980).

14. R. H. Friend, D.D.C. Bradley, and P.D. Townsend, *J. Phys. D*, **20**, 1367 (1987); Furukawa, , *J. Phys. Soc. Jpn.*, **58**, 2976 (1989); K. Fesser, et. al., *Phys. Rev. B*, **27**, 4804 (1983).

15. A. J. Heeger, S. Kivelson, J.R. Schrieffer, W.-P.Su, *Rev. Mod. Phys.*, **60**, 781 (1988).

16. T. A. Geissman, *Principles of Organic Chemistry*, W. H. Freeman, San Francisco (1962).

17. C. Kittell, *Introduction to Solid State physics*, Wiley, New York (1986).

18. J. I. Pankove, *Optical Processes in Semiconductors*, Dover, New York (1971).

19. R. J. Elliot, *Phys. Rev.*, **108**, 1384 (1957).

20. Z. G. Soos, S. Etemad, D.S. Galvao, and S. Ramasesha, *Chem. Phys. Lett.*, **194**, 341 (1992).

21. Z. G. Soos, S. Ramasesha, D.S. Galvao, R.G. Kepler, and S. Etemad, *Synth. Met.*, **54**, 35 (1993).

22. Z. G. Soos, S. Ramasesha, and D.S. Galvao, *Phys. Rev. Lett.*, **71**, 1609 (1993).

23. J. M. Leng, S. Jeglinski, X. Wei, R.E. Brenner, Z.V. Vardeny, F. Guo, and S. Mazumdar, *Phys. Rev. Lett.*, **72**, 156 (1994).

24. S. N. Dixit, Dandan Gao, and S. Mazumdar, *Phys. Rev. B*, **43**, 6781 (1991).

25. Y. Kawabe, et. al., *Phys. Rev. B*, **44**, 6530 (1991).

26. S. Abe, M. Schrieber, W.P. Su, and J. Yu, *Phys. Rev. B*, **45**, 9432 (1992).

27. C. P. Poole, *Electron Spin Resonance*, Wiley, New York (1983).

28. G. E. Pake and T. L. Estle, *The Physical Principles of Electron paramagnetic Resonance*, Benjamin, London (1973).

29. H. P. Gislason, F. Rong and G. D. Watkins, *Phys. Rev. B*, **32**, 6945 (1985).

30. S. D. McGlynn, et. al., *Molecular Spectroscopy of the Triplet State*, Prentice-Hall, Englewood Cliffs, N. Y. (1979).

31. E. L. Frankevich, A.A. Lymarev, I. Sokolik, F.E. Karasz, S. Blumstengel, R.H. Baughman, and H.H. Hörhold, *Phys. Rev. B*, **46**, 9320 (1992).

32. J. W. P. Hsu, et. al., *Phys. Rev. B*, **49**, 712 (1994).

33. S. Kuroda, T. Noguchi, and T. Ohnishi, *Phys. Rev. Lett.*, **72**, 286 (1994).

34. H. A. Mizes and E. M. Conwell, *Phys. Rev. Lett.*, **70**, 1505 (1993).

35. M. Yan, L.J. Rothberg, et. al., in press.

36. Q.-X. Ni, J. Shinar, Z.V. Vardeny, S. Grigoras, Y. Pang, S. Ijadi-Maghsoodi, and T.J. Barton, *Phys. Rev. B*, **44**, 5939 (1991).

37. L. S. Swanson, J. Shinar, and K. Yoshino, *Phys. Rev. Lett.*, **65**, 1140 (1990).

38. L. S. Swanson, et. al., *Phys. Rev. B*, **44**, 10617 (1991).

39. Q.-X. Ni, L.S. Swanson, P.A. Lane, J. Shinar, Y.W. Ding, S. Ijadi-Maghsoodi, and T.J. Barton, *Syn. Met.*, **49-50**, 447 (1992).

40. L. S. Swanson, J. Shinar, A.R. Brown, D.D.C. Bradley, R.H. Friend, P.L. Burn, A. Kraft, and A.B. Holmes, *Phys. Rev. B*, **46**, 15072 (1992).

41. L. S. Swanson, et. al., *Syn. Met.*, **55-57**, 447 (1992).

42. D. D. C. Bradley and R. H. Friend, *J. Phys. Cond. Matt.*, **1**, 3671 (1989).

43. K. E. Ziemelis, A.T. Hussain, D.D.C. Bradley, R.H. Friend, J. Rühe, and G. Wegner *Phys. Rev. Lett.*, **66**, 2231 (1991).

44. M. Yan, L.J. Rothberg, F. Papadimitrakopoulos, M.E. Galvin, and T.M. Miller, *Phys. Rev. Lett.*, **72**, 1104 (1994).

45. Z. V. Vardeny, et. al., to be published.

APPENDIX

EXPERIMENTAL DETAILS

1- When sealing the sample tube end, one should adjust the gas flow until approximately 0.5 to 1 inch of the base of the flame is burning blue. The tube should be held perpendicular to the direction of the flame at the tip of this blue part for best results. If the tube is allowed to get too hot, an irreversible reaction will take place and the tube will no longer be capable of sealing. It is possible to know when the tube is sealed by observing the hollow part creep away from the tube end.

2- The last step in the sealing process is to seal the remaining open end of the glass tube. To do this, simply leave the tube's open end connected to the pump after degassing. Then, bring the blue tip of the oxy-acetylene flame perpendicular to the tube as close to the open end as possible without burning the veeco valve fitting. The tube will collapse separating the sample from the pump. Slowly pull and twist the tube off of the pump while continuously heating the "melted" glass. Once it is off, burn the tail of the seal down to a harmless bump with the torch. Label the sample immediately. Lastly, close the pump off to the separated end of the tube, remove the glass and discard it in the appropriate glass disposal container.

3- Before enabling the laser, the laser water and the laser water pump must be turned on. The laser circuit breaker which also enables the safety lockout on the door and the main power breaker to the laser located on the power supply itself must be turned on. This switch does not put the laser into the lasing mode. Ten to fifteen minutes should elapse before

attempting to put the laser into the lasing mode by pushing the button next to the light which indicates the laser is "ready". It is important to note that this "ready" button is to be ignored and more time should elapse after it switches on before lasing begins otherwise the current will overload and the system will buzz and will have to be shut down immediately. Once the laser is switched into the lasing mode, the wavelength of the laser can be tuned at the back. Lastly, the shutter controller must be enabled to release the safety beam blocker and allow the laser beam free access to the optics and ultimately the sample. Note that the blocker will fall and block the laser beam if the door is opened during operation and the special entry trigger button is not pushed on the lockout box inside the lab or the key enable to the box is not used outside the lab. After shutting off the laser, the water must be allowed to flow using the pump cooling the ion-gas tube for fifteen minutes before it can safely be turned off.

4- Before cooling, the sample is placed in a vacuum insulated continuous flow cryostat. The cold helium gas is drawn from a highly specialized dewar containing liquid helium. This dewar, when empty, can be filled by the experts, specifically Paul Ness, in the cryogenics laboratory in a fairly short turn around time. The filled dewar is then returned to the laboratory and immediately hooked up to the helium gas return line. Care must be taken to insure that the ball valves on the dewar and on the return line are opened at this time. Only then can the five p.s.i. valve on the dewar be returned to the closed position.

The transfer tube must now be prepared for insertion into the dewar and cryostat itself. The first step is to flush the inner capillary of the transfer tube with nitrogen gas in order to insure that all of the moisture from the air inside is removed. This is accomplished by

hooking the N_2 gas over the needle valve and putting a sealing tube over the end which normally goes into the cryostat and pumping the gas through the tube for about ten minutes. Next, the nitrogen gas is removed by repeating the preceding steps with helium gas. Neither the nitrogen or helium gas sources should be removed until overpressure is reached in the capillary.

After pumping the helium gas through for about ten minutes, the transfer tube is inserted into the liquid helium storage dewar. Put it in at first only in the gas above the liquid and pump for a few minutes before lowering it slowly into the tank. The transfer tube should be lowered slowly enough so that the "ping-pong ball" flowmeter on the return line only reads about one inch. Once insertion into the storage dewar is complete, let the pump continue to circulate helium until liquid begins to flow (the helium flowmeter indicates significantly higher flow) and then shut off the pump. After overpressure is reached, take the sealing tube off of the transfer tube end and insert it into the cryostat *slowly and carefully*. There will be one place where it will hang up on the way in (when the tip encounters the narrow part of the cryostat feedthrough). Without much force, wiggle the tube end until it goes in all the way. Screw down the connector. Note that from time to time this connector must be moved up the tube end as it tends to slide down until a proper seal is no longer being made between the teflon O-ring of the transfer tube and the cryostat sealing location.

If the vacuum jacket of the transfer tube is pumped down and the vacuum jacket, which must be continuously pumped during low temperature experiments, is at least 5×10^{-4} Torr, then the pump can be turned on and low temperature experiments can be performed as

soon as the desired temperature is reached. Temperature variation is accessible using the flowmeter valve, the needle valve on the transfer tube and the heater contained within the thermocouple system. In order to read the proper temperature, the thermocouple must be referenced to liquid nitrogen. This reference is located at the back of the magnet and there is a nitrogen dewar there for this purpose which must be filled prior to running.